Original Article

Development and evaluation of a T1 standard brain template for Alzheimer disease

Xiao-Yi Guo[1], Yunjung Chang[2], Yehee Kim[2], Hak Young Rhee[3], Ah Rang Cho[4], Soonchan Park[5], Chang-Woo Ryu[5], Jin San Lee[6], Kyung Mi Lee[7], Wonchul Shin[3], Key-Chung Park[6], Eui Jong Kim[7], Geon-Ho Jahng[5]

[1]Department of Medicine, Graduate School, Kyung Hee University, Seoul, Republic of Korea; [2]Department of Biomedical Engineering, Undergraduate School, College of Electronics and Information, Kyung Hee University, Gyeonggi-do, Republic of Korea; [3]Department of Neurology, Kyung Hee University Hospital at Gangdong, College of Medicine, Kyung Hee University, Seoul, Republic of Korea; [4]Department of Psychiatry, Kyung Hee University Hospital at Gangdong, College of Medicine, Kyung Hee University, Seoul, Republic of Korea; [5]Department of Radiology, Kyung Hee University Hospital at Gangdong, College of Medicine, Kyung Hee University, Seoul, Republic of Korea; [6]Department of Neurology, Kyung Hee University Hospital, College of Medicine, Kyung Hee University, Seoul, Republic of Korea; [7]Department of Radiology, Kyung Hee University Hospital, College of Medicine, Kyung Hee University, Seoul, Republic of Korea

Correspondence to: Geon-Ho Jahng, PhD. Professor of Radiology, Kyung Hee University Hospital at Gangdong, College of Medicine, Kyung Hee University, #892 Dongnam-ro, Gangdong-Gu, Seoul 05278, Republic of Korea. Email: ghjahng@gmail.com.

Background: Patients with Alzheimer disease (AD) and mild cognitive impairment (MCI) have high variability in brain tissue loss, making it difficult to use a disease-specific standard brain template. The objective of this study was to develop an AD-specific three-dimensional (3D) T1 brain tissue template and to evaluate the characteristics of the populations used to form the template.

Methods: We obtained 3D T1-weighted images from 294 individuals, including 101 AD, 96 amnestic MCI, and 97 cognitively normal (CN) elderly individuals, and segmented them into different brain tissues to generate AD-specific brain tissue templates. Demographic data and clinical outcome scores were compared between the three groups. Voxel-based analyses and regions-of-interest-based analyses were performed to compare gray matter volume (GMV) and white matter volume (WMV) between the three participant groups and to evaluate the relationship of GMV and WMV loss with age, years of education, and Mini-Mental State Examination (MMSE) scores.

Results: We created high-resolution AD-specific tissue probability maps (TPMs). In the AD and MCI groups, losses of both GMV and WMV were found with respect to the CN group in the hippocampus ($F>44.60$, $P<0.001$). GMV was lower with increasing age in all individuals in the left ($r=-0.621$, $P<0.001$) and right ($r=-0.632$, $P<0.001$) hippocampi. In the left hippocampus, GMV was positively correlated with years of education in the CN groups ($r=0.345$, $P<0.001$) but not in the MCI ($r=0.223$, $P=0.0293$) or AD ($r=-0.021$, $P=0.835$) groups. WMV of the corpus callosum was not significantly correlated with years of education in any of the three subject groups ($r=0.035$ and $P=0.549$ for left, $r=0.013$ and $P=0.821$ for right). In all individuals, GMV of the hippocampus was significantly correlated with MMSE scores (left, $r=0.710$ and $P<0.001$; right, $r=0.680$ and $P<0.001$), while WMV of the corpus callosum showed a weak correlation (left, $r=0.142$ and $P=0.015$; right, $r=0.123$ and $P=0.035$).

Conclusions: A 3D, T1 brain tissue template was created using imaging data from CN, MCI, and AD participants considering the participants' age, sex, and years of education. Our disease-specific template can help evaluate brains to promote early diagnosis of MCI individuals and aid treatment of MCI and AD individuals.

Keywords: Alzheimer disease (AD); standard brain template; gray and white matter volume; age; years of education

Submitted May 28, 2020. Accepted for publication Jan 08, 2021.
doi: 10.21037/qims-20-710
View this article at: http://dx.doi.org/10.21037/qims-20-710

Introduction

Alzheimer disease (AD), the most prevalent age-related neurodegenerative disease, is clinically characterized by a progressive loss of memory and other cognitive functions. Mild cognitive impairment (MCI) is generally regarded as the intermediate stage between normal cognitive changes with aging and very early dementia.

A brain template or brain atlas provides a standard reference for the assessment of brain structure and function and is an important tool in research and clinical practice. Brain imaging from many individuals can be combined to generate a standard brain template or brain atlas, which is an anatomical representation of the brain showing group-wise or study population global or regional brain features (1). The Montreal Neurological Institute (MNI) brain template is the international standard as defined by the International Consortium of Brain Mapping (ICBM) and is the default T1 template commonly used in structural and functional imaging packages such as Statistical Parametric Mapping (SPM) (https://www.fil.ion.ucl.ac.uk/spm/). However, the MNI template was created from relatively young individuals; therefore, this template may not be useful for analyzing brains obtained from elderly participants or patients with AD because the MNI template does not represent brain tissue atrophy in elderly subjects and AD patients (2). Previous studies have attempted to create several human brain templates for AD using amyloid positron emission tomography (PET) (3), tau PET (4), fluid-attenuated inversion recovery (FLAIR) (5), or T1-weighted imaging with study-specific populations (6). Advances in the understanding of the structural and functional changes in the elderly, MCI, and/or AD brain would be facilitated by the availability of a disease-specific brain template (7).

Voxel-based morphometry (VBM) from conventional T1-weighted images has proved effective in quantifying brain atrophy in MCI and AD and has enabled fairly accurate automated classification of AD patients, MCI patients, and elderly cognitively normal (CN) controls (8). Gray matter volume (GMV) loss is characteristic in patients with MCI and AD (9). Patients with AD exhibit significant GMV reductions, mainly in the hippocampus, parahippocampal gyrus, insula, superior/middle temporal gyrus, thalamus, cingulate gyrus, and superior/inferior parietal lobule (10). White matter volume (WMV) reductions were found predominantly in the temporal lobe, corpus callosum, and inferior longitudinal fasciculus (10). Changes in cognition and loss of GMV and WMV are found in both normal aging and AD (11). Therefore, the pattern of brain tissue volume reduction will help us understand the underlying pathologic mechanisms in AD and potentially can be used as an imaging marker for studies of AD in the future.

Several factors should be considered when brain tissue losses are evaluated in participants with AD, MCI, and normal aging. First, most people with AD are aged 65 years or older. People younger than 65 years can have AD, but they are much less likely to develop the disease than older individuals. As age increases, so does the likelihood of having AD (12). Therefore, older age is one of the greatest risk factors for AD (13,14). Second, almost two-thirds of the population with AD is female. Therefore, being female is one of the greatest risk factors for AD (15). Third, people with fewer years of formal education are at higher risk for AD than those with more years of formal education (12). Some researchers believe that having more years of education builds a "cognitive reserve," which enables individuals to better compensate for changes in the brain that could result in the symptoms of AD or other dementias. Therefore, a low number of years of education is one of the greatest risk factors for AD. Finally, although a case-control study using total intracranial volume (TIV) as measured using magnetic resonance imaging (MRI) found no association between head size and AD, a large brain could have more brain tissue than a small one (16). Therefore, we should take into account age, sex, education level, and TIV when the brain tissue template is created using data from CN, MCI, and AD participants.

Patients with AD and MCI have high variability in brain tissue loss, making it difficult to use a disease-specific standard brain template. The objectives of this study were the following: (I) to develop an AD-specific three-dimensional (3D) T1 brain template, (II) to evaluate the differences in GMV and WMV among the three groups of AD, MCI, and CN used to create our AD template, (III) to evaluate the correlation between GMV and WMV loss with age, years of education, or Mini-Mental State Examination score, and (IV) to evaluate the difference in brain tissue

volumes between our AD template and other published templates in some specific areas of the brain.

Methods

Participants

This study was approved by the institutional review board, and informed consent was obtained from all participants. All participants were prospectively recruited from the neurological center of our institution during four different cohort studies supported by the Korean government. The detailed information regarding the funding sources for the four cohorts is listed in the Acknowledgement.

All participants provided a detailed medical history and underwent neurologic examination, standard neuropsychological testing, and MRI. Cognitive function was assessed using the Seoul Neuropsychological Screening Battery (SNSB) (17), which is a standardized neuropsychological test battery from Korea that covers five cognitive subsets: attention, memory, language, visuospatial function, and frontal/executive function. The SNSB includes the Korean version of the Mini-Mental State Examination (K-MMSE) for global cognitive ability. Brain imaging from each participant was evaluated by two neuroradiologists, with more than 10 years of MRI experience each, to determine any evidence of prior cortical infarctions or other space-occupying lesions.

To create a disease-specific brain template, we included elderly CN, amnestic MCI, and mild and probable AD individuals. Amnestic MCI subjects were identified according to Petersen's criteria (18,19) as follows: (I) cognitive complaints by the patient or caregiver; (II) normal general cognitive function on the K-MMSE; (III) cognitive impairment on objective testing; (IV) normal activities of daily living; and (V) no dementia. Patients with mild and probable AD were defined as those with clinical dementia rating (CDR) scores of 0.5, 1, or 2, according to the criteria of the National Institute of Neurological and Communicative Disorders and Stroke-Alzheimer Disease and Related Disorders Association (20): (I) dementia established by clinical examination and standardized brief mental status examination and confirmed by neuropsychological tests; (II) deficits in two or more areas of cognition; (III) progressive worsening of memory and other cognitive functions; (IV) no disturbance of consciousness; (V) onset between 40 and 90 years of age; and (VI) absence of other systemic or neurologic disorders sufficient to account for progressive cognitive defects. Elderly CN participants were selected from healthy volunteers who did not have a medical history of neurological disease, and who also had a normal brain MRI.

Images were selected from four different cohorts that had been studied by the authors for four different purposes. Participants were prospectively recruited to have the following titled studies: (I) "*Developments and clinical applications of magnetic resonance imaging sequences to early detect Alzheimer disease*" in 120 subjects (Cohort 1); (II) "*Technical developments and those clinical applications of functional MRI techniques to early detect Alzheimer disease*" in 89 subjects (Cohort 2); (III) "*Development of a quantitative susceptibility mapping to amyloid imaging and oxygen metabolism mapping in AD*" in 62 subjects (Cohort 3); and (IV) "*Developments of novel magnetic resonance imaging techniques to image brain metabolites and neurotransmitters*" in 55 subjects (Cohort 4). Therefore, a total of 326 subjects were included in this study. The participants comprised 111 elderly CN participants with no medical history of neurological disease [31 men and 80 women; age: mean (SD), 65 (8.3) years], 101 elderly amnestic MCI patients [33 men and 68 women; 69.7 (7.4) years], and 114 elderly AD patients [22 men and 92 women; 74.7 (8.33) years]. The characteristics of the demographic data of the participants in each cohort are summarized in Table S1. We excluded 32 participants, which included 13 AD, 5 MCI, and 14 CN individuals due to brain abnormalities. A total of 294 subjects were included in this study: 97 in the CN group, 96 in the MCI group, and 101 in the AD group. *Table 1* summarizes the demographic data, results of the neuropsychological tests, and global brain tissue volumes obtained from the segmented 3D T1W images of the individuals.

MRI acquisitions

MRI scans for Cohorts 1 to 4 were acquired for each participant using a 3-T MR system (Achieva, Philips Medical Systems, Best, The Netherlands) equipped with an eight-channel sensitivity encoding head coil. A sagittal structural 3D T1-weighted (T1W) image was acquired using a turbo field echo sequence that is similar to the magnetization-prepared rapid acquisition of gradient echo (MPRAGE) sequence with the following parameters: repetition time (TR) =8.1 ms, echo time (TE) =3.7 ms, flip angle (FA) =8°, field-of-view (FOV) =236×236 mm^2, acquisition voxel size =1×1×1 mm^3, and reconstruction voxel size =1×1×1 mm^3. In addition, T2-weighted turbo-

Table 1 Statistical results of the demographic data, result of the neuropsychological tests, and global segmented brain tissue volumes among the three participant groups with cognitively normal (CN) elderly, amnestic mild cognitive impairment (MCI), and Alzheimer's disease (AD)

Groups	CN[1]	MCI[2]	AD[3]	P value (post-hoc)
Participants	97	96	101	294 (total)
Demographic data and neuropsychologic test				
*Age (years)	65.23±7.61	69.51±7.47	75.28±8.20	F=41.742, P<0.001 [1,2,3]
&Sex (M/F)	31/66	32/64	20/81	χ^2=5.440, P=0.066
	M: 31.96%	M:33.33%	M:19.80%	
	F: 68.04%	F: 66.67%	F: 80.20%	
*Education (years)	9.62±5.17	9.12±4.72	5.68±5.22	F=18.024, P<0.001
#K-MMSE	28 (28 to 29)	27 (26 to 27)	17 (16 to19)	H=187.947, P<0.001 [1,2,3]
CDR	0 (0–0.5)	0.5 (0–0.5)	1 (0.5–1)	N/A
*Global segmented brain tissue volumes				
TIV (mm^3)	1,464.35±170.17	1,463.11±117.13	1,418.30±118.63	F=3.628, P=0.028
Global GMV (mm^3)	599.57±63.90	578.15±51.13	517.42±46.29	F=61.472, P<0.001 [1,2,3]
Global WMV (mm^3)	486.81±95.73	466.76±48.19	428.23±46.97	F=19.390, P<0.001[1,3], [2,3]
Global CSFV (mm^3)	377.97±55.15	418.20±73.93	472.65±65.86	F=52.326, P<0.001 [1,2,3]

*P value by ANOVA with Scheffé test for the post hoc test; &P value by chi-squared test; #P value by Kruskal-Wallis test with Conover method for the post hoc test. Note: the data of age, education-year, TIV, global GMV, global WMV, and global CSF volume are presented as the mean ± standard deviation. K-MMSE scores are listed as median (95% CI for the median). CDR scores are presented as the median (range) value. Results of the post-hoc test listed as: significant difference among the three subject groups as [1,2,3], between the CN and AD as [1,3], between CN and MCI as [1,2], and between MCI and AD as [2,3]. K-MMSE, Korean version of Mini-Mental State Examination Score; CDR, Clinical Dementia Rating; TIV, total intracranial volume; GMV, gray matter volume; WMV, white matter volume; CSFV, cerebrospinal fluid volume.

spin-echo and FLAIR images were acquired to examine any brain malformations.

Imaging processing to create disease-specific brain template

The following post-processing steps were performed to create the disease-specific brain templates using Statistical Parametric Mapping version 12 (SPM12) software (Welcome Department of Imaging Neuroscience, University College, London, UK). The computational anatomy toolbox (CAT12) tool was used to segment and spatially normalize the individual 3D T1W images to the standard brain template (21). During this first step, affine registration was performed with a tissue probability map (TPM) and ICBM space template of East Asian brains provided by SPM12 software. CAT12 segmentation was performed with the brain template Template_1_IXI555_MNI152 provided by the CAT12 tool with the voxel-size for normalized images of 1.5 mm. CAT12 detects white matter hyperintensities by default. In addition, CAT12 can deal with lesions. These lesion areas are not used for segmentation or spatial registration. GMV and WMV volumes were saved into the native space as well as the Diffeomorphic Anatomical Registration Through Exponentiated Lie Algebra optimization tool (DARTEL) space (22) after applying the affine transformation in order to generate the disease-specific brain template.

Second, the SPM12 segmentation option was used to segment individual 3D T1W images again into six tissue types, which included the GM, WM, and cerebrospinal fluid (CSF), skull, soft tissue outside the brain, air, and other material outside of the head, to generate the disease-specific TPMs. During this second segmentation, we also used six different TPMs provided by the SPM12 software. We saved six different tissue types in the native space and DARTEL space. For the warping process, affine regularization was

performed using the ICBM space template of East Asian brains provided by SPM12 software. The DARTEL tool in SPM12 was used to create the AD-specific brain template. Furthermore, the Template-O-Matic tool was used to create the TPM taking into account age and sex (23).

Statistical analyses

Demographic characteristics and results of neuropsychological tests

Demographic data and clinical outcome scores were compared between the three participant groups. Age, TIV, global GMV, global WMV, global CSF volume, and years of education were all normally distributed (P>0.05 by Levene's test). Hence, a one-way analysis of variance (ANOVA) was used to evaluate differences in those variables between the three participant groups. Whenever any significant differences between the participant groups were found, we performed a post hoc test for pairwise comparisons of subgroups according to the Scheffé test. The K-MMSE score was not normally distributed (P<0.05, Levene's test). Hence, the Kruskal-Wallis test was used to compare K-MMSE scores between the three participant groups. The Conover method was used in the post hoc test. We compared the difference in the proportion of sexes between participant groups using the chi-squared test.

Voxel-based comparison of GMV and WMV

After creating the AD-specific standard brain template, CAT12 was again used to segment and spatially normalize the individual 3D T1W image into the created AD-specific standard brain template with an isotropic voxel size of 1.5 mm for the voxel-based analyses of brain tissue volumes. The spatially normalized GMV and WMV were smoothed using a Gaussian kernel of 8×8×8 mm full width at half-maximum for statistical analysis.

First, to compare GMV and WMV between the three participant groups without separating individuals by sex, voxel-wise full factorial one-way analysis of covariance (ANCOVA) was performed with TIV, age, sex, and years of education as covariates. Second, a voxel-based regression analysis was performed for each subject group. Third, to compare GMV and WMV between women and men in each participant group, a voxel-wise two-sample *t*-test was used with TIV, age, and years of education as covariates. A significance level of α=0.01 was applied with correction for multiple comparisons using the family-wise error (FWE) method and clusters with at least 50 contiguous voxels.

Voxel-based multiple regression analysis of GMV or WMV to age

Voxel-based regression analysis for each subject group was performed to evaluate the relationship between GMV or WMV loss and age by adjusting TIV, sex, and education year, without separating individuals. Furthermore, this analysis was repeated without separating the three participant groups. In addition, this analysis was repeated, separating the women and men in each participant group by adjusting TIV and education-year. An FWE-corrected significance level of α =0.01 was applied with clusters of at least 50 contiguous voxels.

ROI-based comparison of GMV and WMV

The atlas-based regions-of-interest (ROIs) were bilaterally defined in the amygdala, anterior cingulate, hippocampus, insula, parahippocampal gyrus, posterior cingulate, precuneus, putamen, and thalamus using WFU_PickAtlas software (https://www.nitrc.org/projects/wfu_pickatlas/). Furthermore, the entire corpus callosum was defined as an ROI representing the white matter area. GMV and WMV were extracted from the defined ROIs. Comparison of ROI values between the left and right areas for each ROI in the CN, MCI, and AD groups were performed using a paired samples *t*-test (Table S2).

The following statistical analyses were performed on the ROI data. First, we compared GMV and WMV between the three participant groups for each ROI, using ANOVA. If there was any significant difference between groups, the Scheffé test was used as the post hoc test. Second, to evaluate the relationship between brain tissue volume loss and age, years of education, and K-MMSE scores in each subject group, Spearman's rank correlation for each subject group was performed. Furthermore, this analysis was repeated with all participant groups. A significance level of α=0.016 was applied (α=0.05 divided by three for each subject group) for each analysis. Finally, to evaluate the difference in brain tissue volumes between our AD template and other published templates (24,25) in each ROI, a summary *t*-test was used. Note that the total brain tissue volumes in our AD template were obtained by adding both GMV and WMV, but not CSF volume.

Results

Participant characteristics

Table 1 summarizes the statistical results for the demographic data, results of the neuropsychological tests, and global segmented brain tissue volumes for the three participant

groups. Age was significantly different between the three groups (F=41.742, P<0.001). The proportions of the two sexes were not significantly different between the three groups (χ^2=5.440, P=0.066). Women accounted for a larger proportion of each subject group. The K-MMSE scores were significantly different between the three participant groups, as expected (H=187.947, P<0.001). Years of education were significantly different between the three groups (F=18.024, P<0.001).

TIV was significantly different between the three groups (F=3.628, P=0.028), but the results of the post hoc test did not show any significant differences between group pairs. The global GMV was significantly different among the three groups (F=61.472, P<0.001), and so were the global WMV (F=19.390, P<0.001) and the global CSF volume (F=52.326, P<0.001).

Brain template

Figure 1 shows the generated AD-specific TPMs, which include the gray matter, white matter, CSF, skull, soft tissue, and air and other substances. We generated three orientations with coronal, sagittal, and axial of the gray matter, white matter, CSF, skull, soft tissue, and air and other substances as the a priori images. Our template provides a spatially varying a priori distribution. The standard recommendation to create a brain template is to use a different step to create the template. First, individual 3D T1 images were segmented into several brain tissues after spatially normalizing them into the ICBM space template of East Asian brains. We created a brain template using DARTEL. Furthermore, after renormalization of individual 3D T1 images into DARTEL space, we created the TPM by considering age.

Voxel-based comparisons of GMV and WMV between the three participant groups

GMV

Figure 2 shows the results of the voxel-based group comparisons of GMV between the three participant groups without separating the sexes (*Figure 2A*), including only women (*Figure 2B*), and including only men (*Figure 2C*). Without separating sexes, GMV in the MCI group showed predominant loss relative to the CN group. In the AD group, relative to the CN and MCI groups, areas of GMV loss extended to the entire brain except the motor and somatosensory cortex areas. Table S3A lists the results of the voxel-based group comparisons of GMV between the three participant groups without separation by sex.

When considering only women, *Figure 2B* shows that the pattern of GMV loss was similar to that without separation by sex because women accounted for the majority of each participant group. In addition, there was no significant difference between the CN and MCI groups. Table S3B lists the results of the voxel-based group comparisons of GMV between the three participant groups for women alone.

When considering only men, *Figure 2C* shows that the areas of GMV loss were much smaller than those in women. In the MCI group compared to the CN group, GMV was lower in the left anterior cingulate. In the AD group compared to the CN group, GMV showed a predominant loss in the medial temporal lobe area and some loss in the frontal and parietal lobe areas. In the AD group compared to the MCI group, GMV showed loss predominantly in the temporal lobe area. Table S3C lists the results of the voxel-based group comparisons of GMV between the three participant groups for men alone.

Comparisons of GMV between the women and men in the CN group showed that females in the CN group had lower GMV compared to CN males. However, GMV loss was not significantly different between men and women in the MCI and AD groups. Furthermore, there was no area in which the GMV in women was greater than that in men for all three groups. Table S3D lists the results of the voxel-based group comparisons of GMV between women and men among the three participant groups.

WMV

Figure 3 shows the results of the voxel-based group comparisons of WMV between the three participant groups without separating the sexes (*Figure 3A*), including only women (*Figure 3B*), and including only men (*Figure 3C*). Without separating the sexes, WMV in the MCI group compared with the CN group showed loss predominantly in the bilateral frontal lobe and right middle temporal gyrus. In the AD group compared with the CN and MCI groups, areas of WMV loss were predominantly in the frontal lobe areas. Table S4A lists the results of the voxel-based group comparisons of WMV between the three participant groups without separation by sex.

When considering only women, *Figure 3B* shows that the patterns of WMV loss in the AD group relative to the CN and MCI groups were similar to those without separation by sex. WMV loss in the MCI group was not significantly different from that in the CN group. Table S4B lists the results of the voxel-based group comparisons of WMV between the three participant groups for women.

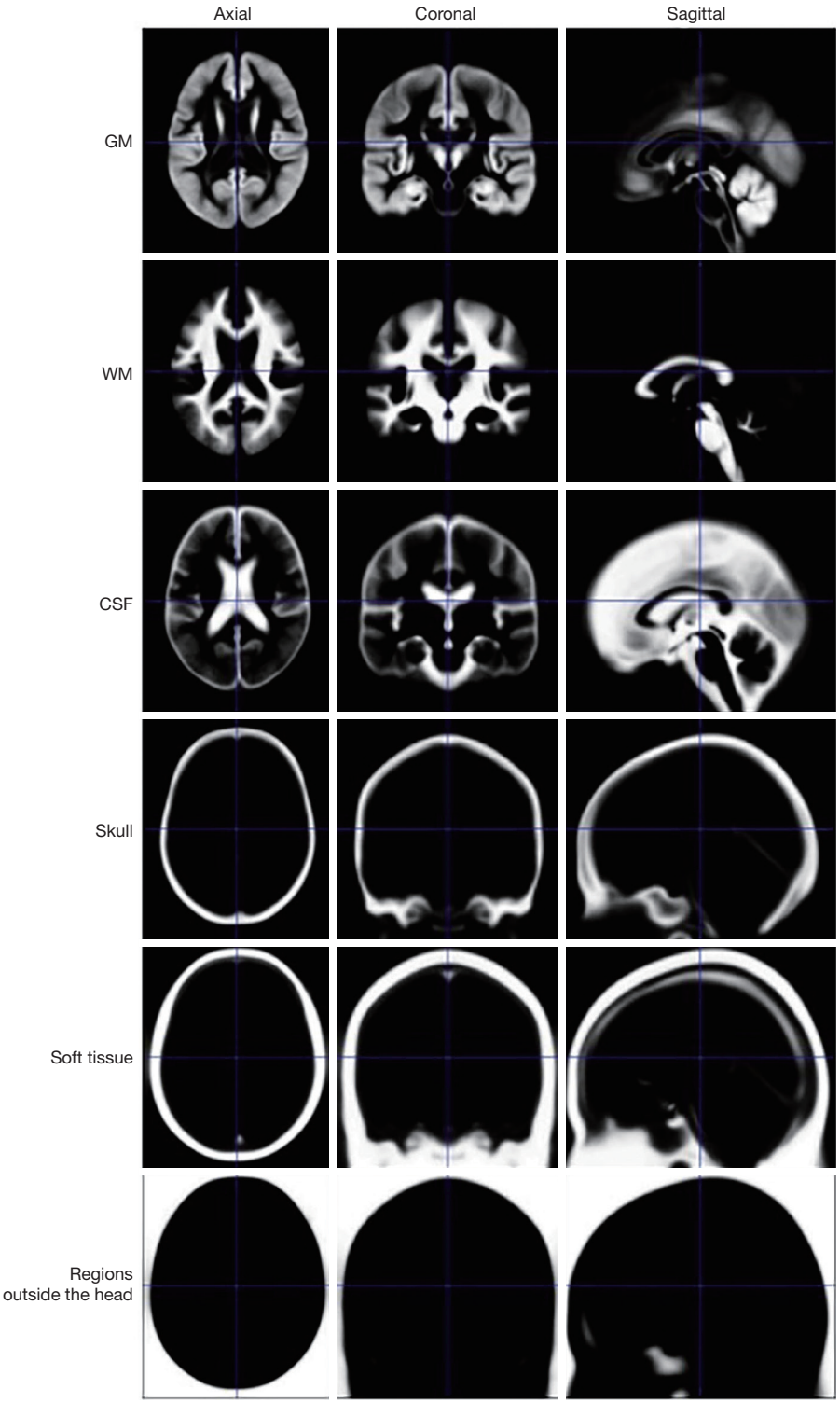

Figure 1 Alzheimer disease-specific tissue probability maps. We display three orientations: axial, coronal, and sagittal sections of gray matter (GM), white matter (WM), cerebrospinal fluid (CSF), skull, soft tissue, and air or other substances. Axial, axial section; Coronal, coronal section; Sagittal, sagittal section.

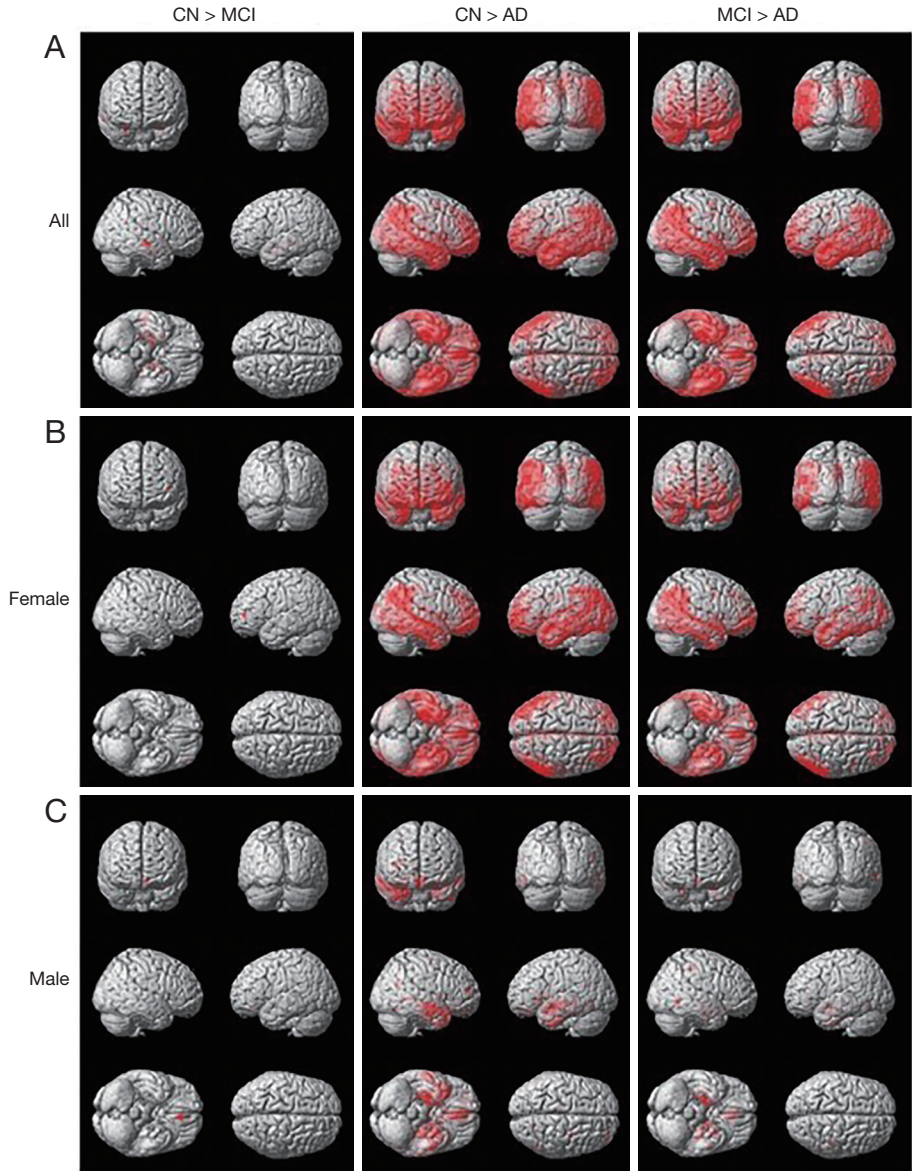

Figure 2 Result of the voxel-based comparisons of gray matter volume (GMV) among the three participant groups without separating gender (A), with only the female group (B), and with only the male group (C). The red color indicates greater GMV in CN than in MCI (left column), in CN than in AD (middle column), and in MCI than in AD (right column). CN, cognitively normal; MCI, amnestic mild cognitive impairment; AD, Alzheimer disease; All, subjects without separating gender.

When considering only men, *Figure 3C* shows that areas of WMV loss were smaller than those in women. In the MCI group relative to the CN group, WMV loss was found in the right frontal lobe and left caudate. In the AD group relative to the CN group, WMV showed loss predominantly in the bilateral frontal lobe, bilateral temporal lobe, and right caudate. In the AD group relative to the MCI group, WMV showed loss predominantly in the bilateral frontal lobe, bilateral temporal lobe, left uncus, and right parietal lobe. Table S4C lists the results of the voxel-based group comparisons of WMV between the three participant groups for men alone.

Comparisons of WMV between the women and men in the CN group showed that CN females had lower WMV in the right middle frontal gyrus and right frontal lobe than CN males. WMV loss in the MCI group was also greater in women than in men in the left midbrain. WMV in the

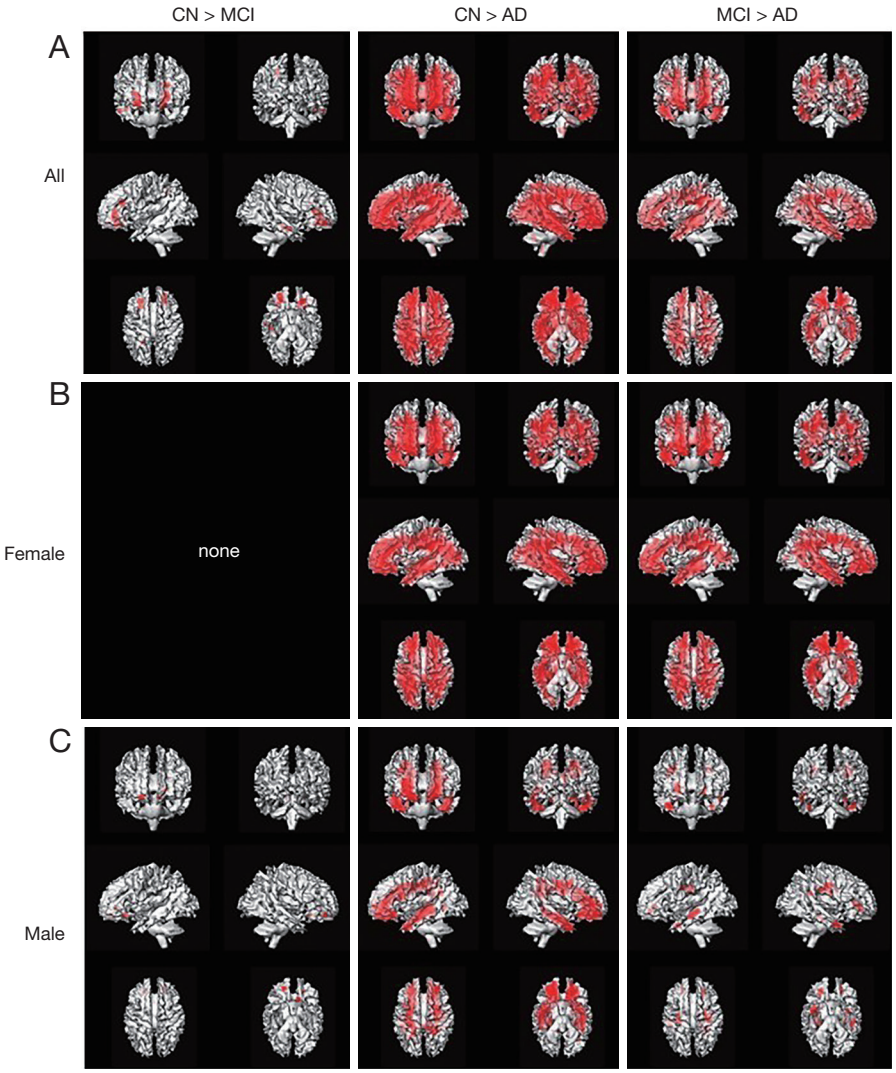

Figure 3 Result of the voxel-based comparisons of white matter volume (WMV) among the three participant groups without separating gender (A), with only the female group (B), and with only the male group (C). The red color indicates greater WMV in CN than in MCI (left column), in CN than in AD (middle column), and in MCI than in AD (right column). The word "none" indicates that there was no significant difference between the two groups. CN, cognitively normal; MCI, amnestic mild cognitive impairment; AD, Alzheimer disease; All, subjects without separating gender.

AD group was not significantly different between men and women. Table S4D lists the results of the voxel-based group comparisons of WMV between women and men among the three participant groups.

Voxel-based multiple regression analyses of brain tissue volume and age

GMV and age

The results of the voxel-based regression analysis revealed that GMV decreased with increasing age for each participant group and all participants together, as shown in *Figure 4*. Without separation by sex (*Figure 4A*), GMV decreased with increasing age in the CN, MCI, and AD groups, and all subjects together. In the CN group, regions of negative correlation were found in the cingulate gyrus, temporal gyrus, and parietal gyrus. In the MCI group, the regions of negative correlation extended to the frontal and occipital lobes. In the AD group, we only found a negative correlation in the cerebellum. Taking all groups together,

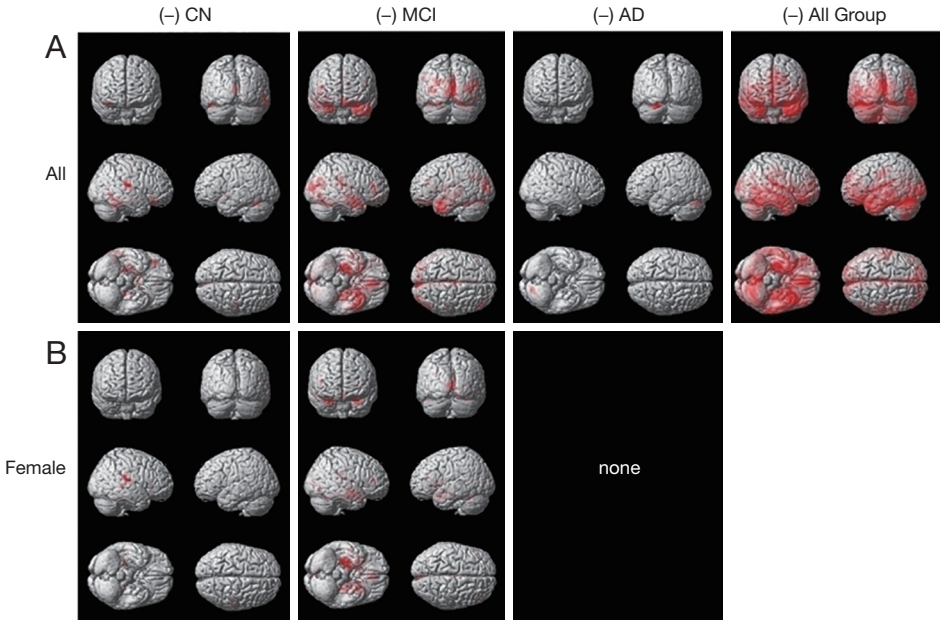

Figure 4 Result of the voxel-based regression analysis of gray matter volume (GMV) to age for each participant group and all groups together without separating gender (A) and with only the female group (B). Note that no associations were observed for the analysis with only the male group. With increasing age, the area of reduction in gray matter volume (GMV) is indicated in red. The negative sign "-" indicates that there was a significantly negative correlation between GMV loss and age. The word "none" indicates that there was no significant correlation between GMV loss and age. CN, cognitively normal; MCI, amnestic mild cognitive impairment; AD, Alzheimer's disease; All, subjects without separating gender; All Group, all subjects with CN, MCI, and AD.

we found GMV loss with increasing age in most brain areas, except the motor cortex area. Table S5A lists the results of the voxel-based regression analysis for GMV and age for each participant group.

When considering only women (*Figure 4B*), GMV decreased with increasing age only in the CN and MCI groups, but not in the AD group. Areas of GMV loss in the CN subject group included the right superior temporal gyrus, right thalamus, right insula, and left occipital lobe. Areas of GMV loss in the MCI subject group extended into the frontal lobe, anterior cingulate, parietal lobe, and occipital lobe. There was no negative correlation between GMV and age in the AD group. There were no positive correlations between GMV and age in any of the three participant groups. Table S5B lists the results of the voxel-based regression analysis for GMV and age for each participant group in women alone.

When considering men alone, there was no correlation between GMV and age in any of the three participant groups.

WMV and age

The results of the voxel-based regression analysis revealed decreased WMV with increasing age for each participant group and all participants together, as shown in *Figure 5*. Without separation by sex (*Figure 5A*), WMV decreased with increasing age in the CN, MCI, and AD groups, and all participants together. In the CN group, areas of negative correlation were found in the left cingulate gyrus and right inferior parietal lobule. In the MCI group, we found a more severe loss of WMV than that in the CN group. The areas of negative correlation further extended to the temporal lobe and parahippocampal gyrus. In the AD group, the areas of negative correlation between WMV and age were much smaller than those in the MCI group. The areas of negative correlation included the anterior cingulate and frontal lobe. Considering all participant groups together, we found WMV loss with increasing age in most brain areas, particularly in the parahippocampal gyrus and frontal lobe. Table S6A lists the results of the voxel-based regression analysis for WMV and age for each participant group.

When considering only women (*Figure 5B*), WMV decreased with increasing age in the CN and MCI groups. In the CN group, areas of negative correlation included the temporal lobe. In the MCI group, areas of negative

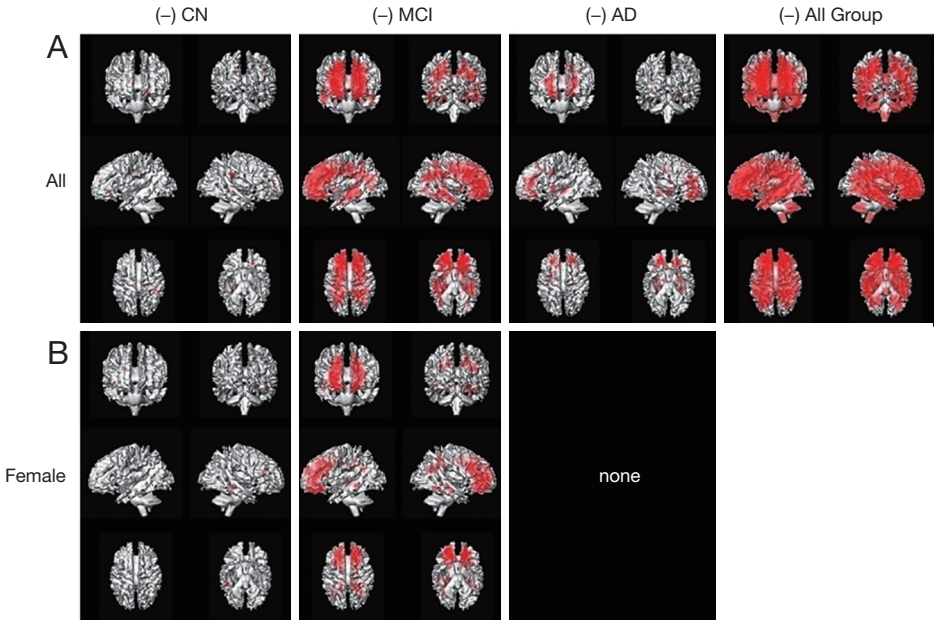

Figure 5 Results of the voxel-based regression analysis of white matter volume (WMV) to age for each participant group and all groups together without separating gender (A) and for only the female group (B). Note that no differences were observed for the analysis with only the male group. With increasing age, the area of reduction in the WMV is indicated in red. The negative sign "–" indicates that there was a significantly negative correlation between WMV loss and age. The word "none" indicates that there was no significant correlation between WMV loss and age. CN, cognitively normal; MCI, amnestic mild cognitive impairment; AD, Alzheimer's disease; All, subjects without separating gender; All Group, all subjects with CN, MCI, and AD.

correlation extended into the frontal lobe, anterior cingulate, parietal lobe, and occipital lobe. In the AD group, there were no areas of negative correlation between WMV and age. Table S6B lists the results of the voxel-based regression analysis for WMV and age for women in each participant group. When considering only men, there was no correlation between WMV and age in any of the three participant groups.

ROI-based analyses

Comparisons of ROI values between the three participant groups

Table 2 lists the results of comparisons of brain tissue volumes between the three participant groups. The GMV of all ROIs were significantly different between the three participant groups ($P<0.001$). GMV was significantly different among the three participant groups in the amygdala, parahippocampal gyrus, hippocampus, and thalamus. WMV was significantly different among the three participant groups in the bilateral parahippocampal gyrus, right posterior cingulate, and left hippocampus.

Correlation between brain tissue volumes and age, years of education, and K-MMSE score in each ROI

Table 3 lists the results of the correlation analysis between the ROI values and age, years of education, and K-MMSE score. First, GMV was found to decrease with increasing age in the CN group for all ROIs except the left and right putamen, in the MCI group for all ROIs, while in the AD group, there was no correlation for all ROIs. The WMV of the corpus callosum did not significantly correlate with age in any of the three participant groups.

Second, years of education in the CN group positively correlated with GMV. GMV in any ROI, except the posterior cingulate, did not significantly correlate with years of education in either the MCI or AD group. WMV of the corpus callosum did not significantly correlate with years of education in any of the three participant groups.

Finally, the MMSE score in the CN group did not correlate with GMV in any ROI. In the MCI group, MMSE scores were significantly correlated with GMV. In the AD group, MMSE scores significantly correlated with GMV in the parahippocampal gyrus and right precuneus. WMV in the corpus callosum did not significantly correlate

Table 2 Results of comparisons of brain tissue volumes among the three participant groups in the specific brain areas

ROI	Side	GMV (mm^3)					WMV (mm^3)				
		CN[1]	MCI[2]	AD[3]	P value*	All	CN[1]	MCI[2]	AD[3]	P value*	All
Amygdala	Lt	598±60	545±90	420±79	F=137.41; P<0.001 [1,2,3]	520±108	84±12	80±15	73±18	F=11.96; P<0.001; [1,3], [2,3]	79±16
	Rt	603±61	550±88	427±83	F=131.10; P<0.001 [1,2,3]	525±108	88±13	85±13	80±20	F=6.47; P=0.002 [1,3], [2,3]	84±16
Parahippocampal Gyrus	Lt	433±40	402±49	327±41	F=152.54; P<0.001 [1,2,3]	387±62	168±21	156±24	133±23	F=58.58; P<0.001 [1,2,3]	152±27
	Rt	433±39	402±51	328±42	F=145.56; P<0.001 [1,2,3]	387±62	194±25	184±27	155±23	F=64.15; P<0.001 [1,2,3]	177±30
Posterior Cingulate	Lt	325±41	313±45	273±38	F=42.63; P<0.001 [1,3], [2,3]	303±47	215±26	208±29	230±34	F=13.87; P<0.001; [1,3], [2,3]	218±31
	Rt	325±38	316±45	273±34	F=49.77; P<0.001; [1,3], [2,3]	304±45	194±25	184±27	155 ±23	F=22.30; P<0.001 [1,2,3]	212±30
Corpus Callosum	Lt	98±10	96±11	94±16	F=1.48; P=0.229	96±13	459±59	443±65	396±53	F=29.90; P<0.001; [1,3], [2,3]	432±65
	Rt	109±12	109±12	107±17	F=0.63; P=0.141	108±14	444±57	428±63	381±50	F=33.02; P<0.001; [1,3], [2,3]	417±63
Anterior Cingulate	Lt	308±37	295±38	257±34	F=50.57; P<0.001; [1,3], [2,3]	286±42	274±38	263±37	230±34	F=37.97; P<0.001; [1,3], [2,3]	256±41
	Rt	298±33	283±37	251±29	F=49.26; P<0.001 [1,2,3]	277±38	304±40	290±43	254±36	F=40.09; P<0.001; [1,3], [2,3]	282±45

Table 2 (*continued*)

Table 2 (*continued*)

ROI	Side	GMV (mm^3)					WMV (mm^3)				
		CN[1]	MCI[2]	AD[3]	P value*	All	CN[1]	MCI[2]	AD[3]	P value*	All
Hippocampus	Lt	501±51	458±68	355±56	F=160.61; P<0.001; [1,2,3]	437±85	205±22	196±24	175±22	F=44.60; P<0.001; [1,2,3]	192±26
	Rt	515±51	470±70	363±64	F=154.29; P<0.001 [1,2,3]	448±89	247±26	238±27	211±25	F=48.02; P<0.001; [1,3], [2,3]	232±30
Insula	Lt	361±35	350±41	307±34	F=57.47; P<0.001; [1,3], [2,3]	339±44	199±24	193±24	174±24	F=29.32; P<0.001; [1,3], [2,3]	188±26
	Rt	358±38	343±40	302±32	F=60.00; P<0.001 [1,2,3]	334±43	134±15	130±15	118±14	F=31.18; P<0.001; [1,3], [2,3]	127±16
Precuneus	Lt	313±31	301±35	266±33	F=51.56; P<0.001 [1,2,3]	293±38	183±24	175±24	158±23	F=28.36; P<0.001; [1,3], [2,3]	172±26
	Rt	304±30	294±33	260±34	F=49.78; P<0.001; [1,3], [2,3]	286±37	209±29	201±28	178±28	F=32.46; P<0.001; [1,3], [2,3]	196±31
Putamen	Lt	370±42	356±39	333±42	F=20.28; P<0.001; [1,3], [2,3]	353±44	267±30	260±28	244±31	F=14.19; P<0.001; [1,3], [2,3]	257±31
	Rt	380±41	365±43	344±46	F=17.00; P<0.001; [1,3], [2,3]	362±46	265±33	259±33	238±34	F=17.94; P<0.001; [1,3], [2,3]	254±35
Thalamus	Lt	416±37	393±51	355±46	F=46.21; P<0.001 [1,2,3]	387±51	226±27	226±31	217±30	F=2.75; P=0.066	223±30
	Rt	421±45	396±58	351±51	F=45.93; P<0.001 [1,2,3]	389±59	244±31	245±31	237±35	F=1.78; P=0.171	242±32

*P value by ANOVA with Scheffé for the post hoc test. Note: The data of gray matter volume (GMV) and white matter volume (WMV) are presented as the mean ± standard deviation. Results of the post-hoc test listed as: significant difference among the three subject groups as [1,2,3], between the CN and AD as [1,3], and between MCI and AD as [2,3]. All, all subjects with cognitively normal (CN), amnestic mild cognitive impairment (MCI), and Alzheimer's disease (AD); Rt, right; Lt, left.

Table 3 Results of rank correlation analysis between brain tissue volumes and age, education-year, and K-MMSE in each area

ROI	Side		CN	MCI	AD	All
Amygdala	Lt	Age	−0.378/0.001	−0.670/0.001	−0.222/0.026	−0.614/<0.001
		Education	0.377/0.001	0.285/0.005	0.0756/0.452	0.405/<0.001
		K-MMSE	0.067/0.512	0.538/0.001	0.174/0.082	0.712/<0.001
	Rt	Age	−0.444/0.001	−0.624/0.001	−0.127/0.205	−0.605/<0.001
		Education	0.334/0.001	0.227/0.026	0.050/0.617	0.371/<0.001
		K-MMSE	0.0706/0.492	0.562/0.001	0.262/0.008	0.712/<0.001
Parahippocampal Gyrus	Lt	Age	−0.526/0.001	−0.681/0.001	−0.223/0.025	−0.650/<0.001
		Education	0.377/0.001	0.270/0.008	0.153/0.128	0.424/<0.001
		K-MMSE	0.113/0.270	0.529/0.001	0.280/0.005	0.734/<0.001
	Rt	Age	−0.528/0.001	−0.661/0.001	−0.198/0.047	−0.641/<0.001
		Education	0.300/0.003	0.303/0.003	0.120/0.232	0.398/<0.001
		K-MMSE	0.076/0.461	0.537/0.001	0.283/0.004	0.727/<0.001
Posterior Cingulate	Lt	Age	−0.526/0.001	−0.430/0.001	−0.209/0.036	−0.516/<0.001
		Education	0.239/0.018	0.120/0.246	0.280/0.005	0.333/<0.001
		K-MMSE	−0.0248/0.809	0.271/0.008	0.209/0.036	0.481/<0.001
	Rt	Age	−0.504/0.001	-0.506/<0.001	−0.251/0.011	−0.562/<0.001
		Education	0.276/0.006	0.154/0.134	0.310/0.002	0.372/<0.001
		K-MMSE	0.010/0.924	0.266/0.009	0.276/0.005	0.517/<0.001
Corpus Callosum	Lt	Age	−0.110/0.283	−0.081/0.434	0.132/0.187	−0.059/0.314
		Education	0.074/0.474	−0.043/0.677	−0.030/0.770	0.035/0.549
		K-MMSE	−0.042/0.680	0.120/0.244	0.102/0.312	0.142/0.015
	Rt	Age	−0.017/0.866	−0.105/0.309	0.161/0.109	0.0031/<0.001
		Education	−0.050/0.630	0.033/0.749	−0.053/0.597	0.013/0.821
		K-MMSE	−0.038/0.712	0.176/0.087	0.067/0.502	0.123/0.035
Anterior Cingulate	Lt	Age	−0.455/<0.001	−0.472/<0.001	−0.148/0.138	−0.523/<0.001
		Education	0.351/<0.001	0.127/0.216	0.284/0.004	0.379/<0.001
		K-MMSE	0.102/0.322	0.357/<0.001	0.265/0.007	0.547/<0.001
	Rt	Age	−0.373/<0.001	−0.429/<0.001	−0.149/0.137	−0.470/<0.001
		Education	0.270/0.008	0.116/0.260	0.209/0.036	0.324/<0.001
		K-MMSE	0.047/0.647	0.322/0.001	0.265/0.007	0.536/<0.001

Table 3 (*continued*)

Table 3 (*continued*)

ROI	Side		CN	MCI	AD	All
Hippocampus	Lt	Age	−0.529/<0.001	−0.652/<0.001	−0.096/0.341	−0.621/<0.001
		Education	0.345/0.001	0.223/0.0293	−0.021/0.835	0.371/<0.001
		K-MMSE	0.0528/0.608	0.514/<0.001	0.157/0.117	0.710/<0.001
	Rt	Age	−0.477/<0.001	−0.675/<0.001	−0.164/0.101	−0.632/<0.001
		Education	0.213/0.036	0.144/0.163	0.029/0.773	0.332/<0.001
		K-MMSE	−0.001/0.996	0.404/<0.001	0.157/0.116	0.680/<0.001
Insula	Lt	Age	−0.356/<0.001	−0.544/<0.001	−0.097/0.335	−0.521/<0.001
		Education	0.219/0.031	0.216/0.035	0.184/0.065	0.361/<0.001
		K-MMSE	0.101/0.327	0.400/<0.001	0.259/0.009	0.589/<0.001
	Rt	Age	−0.537/<0.001	−0.536/<0.001	−0.173/0.084	−0.568/<0.001
		Education	0.328/0.001	0.153/0.137	0.218/0.029	0.367/<0.001
		K-MMSE	0.133/0.196	0.372/<0.001	0.284/0.004	0.594/<0.001
Precuneus	Lt	Age	−0.476/<0.001	−0.555/<0.001	−0.059/0.555	−0.528/<0.001
		Education	0.218/0.032	0.196/0.055	0.121/0.227	0.323/< 0.001
		K-MMSE	0.067/0.518	0.480/<0.001	0.183/0.067	0.584/<0.001
	Rt	Age	−0.505/<0.001	−0.528/<0.001	−0.032/0.753	−0.518/<0.001
		Education	0.321/0.001	0.154/0.134	0.150/0.133	0.339/<0.001
		K-MMSE	0.115/0.261	0.448/<0.001	0.310/0.002	0.587/<0.001
Putamen	Lt	Age	0.008/0.937	−0.305/0.003	−0.147/0.143	−0.283/<0.001
		Education	0.096/0.348	0.056/0.590	−0.012/0.909	0.151/0.010
		K-MMSE	−0.025/0.811	0.269/0.008	0.100/0.318	0.347/<0.001
	Rt	Age	−0.025/0.805	−0.324/0.001	−0.142/0.157	−0.290/<0.001
		Education	0.154/0.133	0.127/0.216	0.054/0.595	0.206/<0.001
		K-MMSE	0.025/0.806	0.268/0.008	0.150/0.134	0.350/<0.001
Lt Thalamus	Lt	Age	−0.400/<0.001	−0.376/<0.001	−0.245/0.014	−0.522/<0.001
		Education	0.158/0.123	0.011/0.919	0.073/0.470	0.214/<0.001
		K-MMSE	0.033/0.745	0.176/0.087	0.059/0.555	0.457/<0.001
	Rt	Age	−0.460/<0.001	−0.378/<0.001	−0.241/0.015	−0.537/<0.001
		Education	0.149/0.144	−0.022/0.830	0.146/0.145	0.218/<0.001
		K-MMSE	0.037/0.720	0.209/0.041	0.091/0.367	0.466/<0.001

*(rho/P value) Spearman's coefficient of rank correlation. All, all participant groups with cognitively normal (CN), amnestic mild cognitive impairment (aMCI), and Alzheimer's disease (AD). K-MMSE, Korean version of Mini-Mental State Examination Score; Rt, right; Lt, left.

Table 4 Summary of comparisons of total brain tissue volumes between templates in each area

ROIs	Brain tissue volume (mm^3, mean ± SD)				
	Our AD template	Chinese	P value*	Caucasian	P value**
L Parahippocampal Gyrus	539±85	6,424±653	P<0.001	5,453±757	P<0.001
R Parahippocampal Gyrus	565±88	5,073±495	P<0.001	5,694±610	P<0.001
L Hippocampus	629±105	3,641±447	P<0.001	3,557±446	P<0.001
R Hippocampus	680±111	3,539±400	P<0.001	3,574±368	P<0.001
L Insula	528±64	8,502±839	P<0.001	9,233±1,184	P<0.001
R Insula	462±56	7,318±607	P<0.001	8,493±1,128	P<0.001
L Precuneus	465±61	12,137±1522	P<0.001	13,205±1,607	P<0.001
R Precuneus	482±65	10,995±1248	P<0.001	11,848±1,327	P<0.001
L Putamen	610±64	4,419±573	P<0.001	3,010±639	P<0.001
R Putamen	616±67	3,691±436	P<0.001	2,580±327	P<0.001

P value* by the summary *t*-test of the brain tissue volume in each area between our AD template and Chinese. P value** by the summary *t*-test of the brain tissue volume in each area between our AD template and Caucasian. Note: The brain tissue volume of our AD template consists of GMV and WMV only without CSF volume.

with MMSE scores in any of the three participant groups.

Comparisons of brain tissue volumes between three different AD templates

Table 4 lists the results of comparisons of total brain tissue volumes between our AD template and two other templates: templates created with a Chinese population (24) or created with a Caucasian population (25) for each ROI. Compared with the two other templates, the brain tissue volumes of our AD template were significantly smaller in all ROIs.

Discussion

Importance of an AD-specific brain template

In this study, we developed an AD-specific brain template using 3D T1WI obtained using a 3-T MRI system with a relatively larger subject population, including CN, MCI, and AD groups. Furthermore, we evaluated the characteristics of the participants by using group comparisons of demographic data, neuropsychological data, and global brain tissue volume, as listed in *Table 1*. Both the CN and MCI groups were younger than the AD group because we included relatively young people in both the CN and MCI groups. This may be a limitation of our template. Women comprised the majority (68% of CN, 66% of MCI, and 80% of AD), similar to the proportion of patients with AD who are female, which is close to two thirds (26). The years of education were lowest in the AD group, which supports the finding that people with more education have a lower incidence of AD (27). In general, MMSE scores between the CN and MCI groups were similar, but in this study, the K-MMSE scores in the MCI group were significantly lower than those in the CN group because we included relatively young people in the CN group compared with those in the MCI group. This is another limitation of our template. For segmented brain tissue volumes, the global GMV loss seen in the aMCI and AD groups indicates that the global GMV values decreased with increasing disease severity. The global WMV loss in the AD group also supported that global WMV values decreased with increasing disease severity. Finally, the global CSF volume was highest in the AD group, indicating that global CSF volumes increased with increasing disease severity.

Researchers have generated several brain templates, such as the MNI152 template (25), Chinese 2020 template (28), and templates of KNE96 using 96 Korean normal elderly subjects (2), and Korean78 using 78 Korean normal elderly subjects (29). First, the MNI152 template was generated using 152 young Caucasian healthy subjects, which is currently used as an international standard brain template in the SPM imaging package unadjusted for age. Second, the Chinese 2020 template was created using 2,020 Chinese

Table 5 Comparisons of the demographic characteristics of published brain templates

Template name	race	N	Group	Mean MMSE score (range)	Mean age (year) (range)	Sex, M/F	Mean education (year)	Mean global TIV (cm^3)	Mean global GMV (cm^3)	Mean global WMV (cm^3)
This paper	Korean	294	CN 97; MCI 96; AD 101	23.7 [2–30]	70.1 [49–92]	83/211	8.10	1,448.12	564.36	423.36
[26] Chinese 2020	Chinese	2,020	HC	N/A	42.4 [20–75]	946/1,074	N/A	N/A	N/A	N/A
[2] KNE96	Korean	96	HC-elderly	N/A	M: 69.5 (60-); F: 70.1 (60-)	48/48	N/A	1614	N/A	N/A
[23] MNI 152	Caucasian	152	HC	N/A	[18–90]	N/A	N/A	N/A	N/A	N/A
[29] MNI 305	Caucasian	305	HC	N/A	23.4	239/66	N/A	N/A	N/A	N/A
[30] ICBM 452	Caucasian	452	HC	N/A	N/A	262/190	N/A	N/A	N/A	N/A
Colin27	Caucasian	1	HC	N/A	N/A	N/A	N/A	N/A	N/A	N/A
French (2009)	French	1	HC	N/A	45	Male	N/A	N/A	N/A	N/A
[22] Chinese_56	Chinese	56	HC	N/A	24.46 [21–29]	Male	N/A	N/A	N/A	N/A
[27] Korea78	Korean	78	HC	N/A	44.6 [18–77]	49/29	N/A	N/A	N/A	N/A
[31] Alzheimer's disease	Caucasian	46	HC-elderly20; AD 26	20.0	72.4; 75.8	12/14; 12/8	15.2; 15.4	N/A	N/A	N/A

N, number of subjects; MMSE, Mini-Mental State Examination; M/F, male/female; TIV, total intracranial volume; GMV, gray matter volume; WMV, white matter volume; CN, cognitively normal elderly; MCI, mild cognitive impairment; AD, Alzheimer's disease; HC, healthy control.

healthy subjects. Normal Korean elderly subjects were used to create the brain templates of KNE96 (2) and Korean78 (29) templates. However, those templates were generated using only healthy control subjects. Our created template is different from the others. We included normal elderly, MCI, and AD patients to create this template. In addition, we adjusted for age. We also created TPM for gray matter, white matter, and CSF. Therefore, our template can be used to evaluate the normal elderly, MCI, and AD brains for gray matter and white matter degeneration, and our template can be the gold standard for evaluating dementia in Asian populations. Several previous studies have created a standard brain template using 3D T1 images (29). It is important to generate a standard TPM to improve brain tissue segmentation.

Since the Talairach and Tournoux atlas (30) have come out, many brain templates have been constructed based on age, race, or specific disease. *Table 5* summarizes the demographic characteristics of several published brain templates. The standard brain templates of MNI152 (25), MNI305 (31), and ICBM452 (32) were based on young healthy Caucasians and were the most generally used in some popular neuroimaging analysis packages. When we compared the TIV values between KNE96 (2) constructed using Korean population data and ours, the TIV did not significantly differ from that in our CN elderly individuals (P=0.1187), although ours was smaller than that of the other. As shown in *Table 4*, the brain tissue volume in every ROI was significantly smaller in our templates than in the Chinese_56 template (24) and Caucasian template (25). This could be related to the fact that, first, the ROI value in each area was only included in GMV and WMV without CSF volume in our study. Second, the ROI value in each area was small due to the elderly and patient population in our study compared to other templates that used healthy controls. Researchers have developed an AD template (33) using both healthy control and AD patients, but a much smaller population than our template.

Evaluation of brain alteration in MCI

MCI is usually very difficult to distinguish from CN based on structural MRI because brain tissue atrophy in the MCI stage is limited to the sulcus gyrus. One of the most important questions in dementia studies is whether it is possible to separate MCI from CN using any neuroimaging modality. With this question in mind, we also wondered whether our AD-specific brain template could be helpful in analyzing neuroimaging data. Although it may be difficult to separate MCI from CN using structural MR images, our standard brain template may be helpful in evaluating MCI subjects. In this study, the voxel-based comparison of GMV between the CN and MCI groups showed that GMV loss in the MCI group was predominantly in the temporal lobe, including the middle and medial temporal lobe, amygdala, and parahippocampal gyri relative to the CN group (Table S3). Furthermore, the voxel-based comparison of WMV between the CN and MCI groups showed that WMV loss in the MCI group was predominantly in the temporal and frontal lobes relative to the CN group (Table S4). Our results support the notion that brain tissue loss starts in the temporal lobe in AD (34). WMV loss in the frontal area may explain the loss of frontal function, consistent with a previous study that showed that frontal function was lost in early-stage AD (35). Based on this result, our brain template can be used to evaluate the early stages of dementia. Our brain template may be used to evaluate brain alterations in MCI participants to promote early detection and earlier therapeutic opportunities for MCI.

Modeling age-dependent brain tissue loss in MCI and AD

To evaluate the characteristics of populations used in our brain template, we performed a correlation analysis between brain tissue volumes and age using voxel-based and ROI-based analyses. The GMV was found to decrease with increasing age in both the CN and MCI groups (Table S5). WMV was also found to decrease with increasing age in both the CN and MCI groups (Table S6). GMV and WMV losses in the CN group with increasing age were limited to some areas in the temporal, frontal, and limbic lobes, as shown in *Figure 4*. Dramatically more brain areas demonstrated GMV and WMV losses in the MCI group. This indicates that it may no longer be a normal physiological brain tissue volume reduction related to age. In MCI, the influence of AD-like pathological factors, such as the deposition and accumulation of beta-amyloid precursor protein (36) and hyperphosphorylated tau protein (37), may already be prominent in the brain. In AD, GMV loss showed limited association with age, indicating that the GMV loss had already occurred in AD. In all participants, GMV and WMV losses were associated with increasing age in most brain areas shown in *Figure 4*. Therefore, our template appears suitable to model age-dependent brain tissue loss in patients with MCI and AD.

A previous cross-sectional study showed that the K-MMSE score in AD patients correlated with brain volume reduction loss (38). Furthermore, a longitudinal study showed that the decline in the K-MMSE score strongly correlated with cortical GMV loss (39). In addition, other previous studies showed a correlation between the hippocampal volume and the MMSE score in the cross-sectional data of AD patients (40) in the longitudinal study of patients with MCI (41).

Limitations

This study had several limitations. First, we did not directly compare our AD-specific standard brain template with the existing standard brain template. It is not easy to compare two standard templates generated from different populations. In addition, it is difficult to find an AD-specific standard brain template generated by using CN, MCI, and AD participant groups. Second, we did not incorporate the genetic information of apolipoprotein E alleles during template creation. It would be more informative if this information is added to the standard brain template. Finally, the age of the AD group was relatively older than that of the CN group. Therefore, although we considered age as a covariate to make the template, it would be better to have exactly matched age among the three participant groups.

Conclusions

We created a 3D T1 brain template using CN, MCI, and AD participants, taking age, sex, and years of education into consideration. We also demonstrated the suitable characteristics of the populations used in the template, such as GMV and WMV losses in the AD and MCI groups relative to the CN group, and GMV loss with increasing age and decreasing years of education. Therefore, our disease-specific template would help evaluate brains in healthy and MCI individuals for early diagnosis and identify MCI individuals for treatment. Furthermore, our AD-specific brain template could be applied for the accurate registration and subsequent analysis of other images, such as PET or single-photon emission computed tomography

data, and other neuroimaging data, such as functional MRI obtained from CN, MCI, and AD individuals. Our AD-specific brain template will be a useful tool for the evaluation of brain tissue loss in patients with dementia. The template developed in this article will be available from the corresponding author upon request.

Acknowledgments

Funding: This work was supported by: (I) the grant of the Korean Health 21 R&D Project, Ministry of Health & Welfare, Republic of Korea [grant number A062284, GHJ], titled "Developments and Clinical Applications of Magnetic Resonance Imaging Sequences to Early Detect Alzheimer's Disease"; (II) the grant of the Korean Health Technology R&D Project, Ministry for Health, Welfare & Family Affairs, Republic of Korea [grant number A092125, GHJ], titled "Technical developments and those clinical applications of functional MRI techniques to early detect Alzheimer's disease"; (III) the grant of the Korean Health Technology R&D Project, Ministry of Health & Welfare, Republic of Korea [grant number HI11C1238 or A111282, GHJ], titled "Development of a Quantitative Susceptibility Mapping to Amyloid Imaging and Oxygen Metabolism Mapping in Alzheimer's Disease"; (IV) The Basic Science Research Program through the National Research Foundation of Korea (NRF) grant funded by the Korea government (MSIP) [grant number 2014R1A2A2A01002728, GHJ], titled "Developments of Novel Magnetic Resonance Imaging Techniques To Image Brain Metabolites and Neurotransmitters"; (V) The Convergence of Conventional Medicine and Traditional Korean Medicine R&D program funded by the Ministry of Health & Welfare through the Korea Health Industry Development Institute (KHIDI) grant number [HI16C2352, GHJ]; (VI) This study was supported by the National Research Foundation of Korea (NRF) grant funded by Ministry of Science and ICT (No. 2020R1A2C1004749, GHJ), Republic of Korea.

Footnote

Conflicts of Interest: All authors have completed the ICMJE uniform disclosure form (available at http://dx.doi.org/10.21037/qims-20-710). The authors have no conflicts of interest to declare.

Ethical Statement: This study was approved by the institutional review board, and informed consent was obtained from all participants.

References

1. Dickie DA, Shenkin SD, Anblagan D, Lee J, Blesa Cabez M, Rodriguez D, Boardman JP, Waldman A, Job DE, Wardlaw JM. Whole Brain Magnetic Resonance Image Atlases: A Systematic Review of Existing Atlases and Caveats for Use in Population Imaging. Front Neuroinform 2017;11:1.
2. Lee H, Yoo BI, Han JW, Lee JJ, Oh SY, Lee EY, Kim JH, Kim KW. Construction and Validation of Brain MRI Templates from a Korean Normal Elderly Population. Psychiatry Investig 2016;13:135-45.
3. Kang SK, Seo S, Shin SA, Byun MS, Lee DY, Kim YK, Lee DS, Lee JS. Adaptive template generation for amyloid PET using a deep learning approach. Hum Brain Mapp 2018;39:3769-78.
4. Sun X, Liang S, Fu L, Zhang X, Feng T, Li P, Zhang T, Wang L, Yin X, Zhang W, Hu Y, Liu H, Zhao S, Nie B, Xu B, Shan B. A human brain tau PET template in MNI space for the voxel-wise analysis of Alzheimer's disease. J Neurosci Methods 2019;328:108438.
5. Firbank MJ, Blamire AM, Krishnan MS, Teodorczuk A, English P, Gholkar A, Harrison R, O'Brien JT. Atrophy is associated with posterior cingulate white matter disruption in dementia with Lewy bodies and Alzheimer's disease. Neuroimage 2007;36:1-7.
6. Thompson P, Mega MS, Toga AW. Disease-Specific Probabilistic Brain Atlases. Proc IEEE Comput Soc Conf Comput Vis Pattern Recognit 2000;2000:227-34.
7. Xie W, Richards JE, Lei D, Zhu H, Lee K, Gong Q. The construction of MRI brain/head templates for Chinese children from 7 to 16 years of age. Dev Cogn Neurosci 2015;15:94-105.
8. Ferreira LK, Rondina JM, Kubo R, Ono CR, Leite CC, Smid J, Bottino C, Nitrini R, Busatto GF, Duran FL, Buchpiguel CA. Support vector machine-based

classification of neuroimages in Alzheimer's disease: direct comparison of FDG-PET, rCBF-SPECT and MRI data acquired from the same individuals. Braz J Psychiatry 2017;40:181-91.
9. Jahng GH, Lee DK, Lee JM, Rhee HY, Ryu CW. Double inversion recovery imaging improves the evaluation of gray matter volume losses in patients with Alzheimer's disease and mild cognitive impairment. Brain Imaging Behav 2016;10:1015-28.
10. Guo X, Wang Z, Li K, Li Z, Qi Z, Jin Z, Yao L, Chen K. Voxel-based assessment of gray and white matter volumes in Alzheimer's disease. Neurosci Lett 2010;468:146-50.
11. Toepper M. Dissociating Normal Aging from Alzheimer's Disease: A View from Cognitive Neuroscience. J Alzheimers Dis 2017;57:331-52.
12. Alzheimer's A. 2016 Alzheimer's disease facts and figures. Alzheimers Dement 2016;12:459-509.
13. Humayun H, Yao J. Imaging the aged brain: pertinence and methods. Quant Imaging Med Surg 2019;9:842-57.
14. Cui D, Zhang L, Zheng F, Wang H, Meng Q, Lu W, Liu Z, Yin T, Qiu J. Volumetric reduction of cerebellar lobules associated with memory decline across the adult lifespan. Quant Imaging Med Surg 2020;10:148-59.
15. Alzheimer's A. 2014 Alzheimer's disease facts and figures. Alzheimers Dement 2014;10:e47-92.
16. Edland SD, Xu Y, Plevak M, O'Brien P, Tangalos EG, Petersen RC, Jack CR Jr. Total intracranial volume: normative values and lack of association with Alzheimer's disease. Neurology 2002;59:272-4.
17. Ahn HJ, Chin J, Park A, Lee BH, Suh MK, Seo SW, Na DL. Seoul Neuropsychological Screening Battery-dementia version (SNSB-D): a useful tool for assessing and monitoring cognitive impairments in dementia patients. J Korean Med Sci 2010;25:1071-6.
18. Petersen RC, Smith GE, Waring SC, Ivnik RJ, Tangalos EG, Kokmen E. Mild cognitive impairment: clinical characterization and outcome. Arch Neurol 1999;56:303-8.
19. Petersen RC, Doody R, Kurz A, Mohs RC, Morris JC, Rabins PV, Ritchie K, Rossor M, Thal L, Winblad B. Current concepts in mild cognitive impairment. Arch Neurol 2001;58:1985-92.
20. McKhann G, Drachman D, Folstein M, Katzman R, Price D, Stadlan EM. Clinical diagnosis of Alzheimer's disease: report of the NINCDS-ADRDA Work Group under the auspices of Department of Health and Human Services Task Force on Alzheimer's Disease. Neurology 1984;34:939-44.
21. Seiger R, Ganger S, Kranz GS, Hahn A, Lanzenberger R. Cortical Thickness Estimations of FreeSurfer and the CAT12 Toolbox in Patients with Alzheimer's Disease and Healthy Controls. J Neuroimaging 2018;28:515-23.
22. Ashburner J. A fast diffeomorphic image registration algorithm. Neuroimage 2007;38:95-113.
23. Wilke M, Holland SK, Altaye M, Gaser C. Template-O-Matic: a toolbox for creating customized pediatric templates. Neuroimage 2008;41:903-13.
24. Tang Y, Hojatkashani C, Dinov ID, Sun B, Fan L, Lin X, Qi H, Hua X, Liu S, Toga AW. The construction of a Chinese MRI brain atlas: a morphometric comparison study between Chinese and Caucasian cohorts. Neuroimage 2010;51:33-41.
25. Mazziotta J, Toga A, Evans A, Fox P, Lancaster J, Zilles K, Woods R, Paus T, Simpson G, Pike B, Holmes C, Collins L, Thompson P, MacDonald D, Iacoboni M, Schormann T, Amunts K, Palomero-Gallagher N, Geyer S, Parsons L, Narr K, Kabani N, Le Goualher G, Boomsma D, Cannon T, Kawashima R, Mazoyer B. A probabilistic atlas and reference system for the human brain: International Consortium for Brain Mapping (ICBM). Philos Trans R Soc Lond B Biol Sci 2001;356:1293-322.
26. Alzheimer's A. 2018 Alzheimer's disease facts and figures. Alzheimer's & Dementia 2018;14:367-429.
27. Meng X, D'Arcy C. Education and dementia in the context of the cognitive reserve hypothesis: a systematic review with meta-analyses and qualitative analyses. PLoS One 2012;7:e38268.
28. Liang P, Shi L, Chen N, Luo Y, Wang X, Liu K, Mok VC, Chu WC, Wang D, Li K. Construction of brain atlases based on a multi-center MRI dataset of 2020 Chinese adults. Sci Rep 2015;5:18216.
29. Lee JS, Lee DS, Kim J, Kim YK, Kang E, Kang H, Kang KW, Lee JM, Kim JJ, Park HJ, Kwon JS, Kim SI, Yoo TW, Chang KH, Lee MC. Development of Korean standard brain templates. J Korean Med Sci 2005;20:483-8.
30. Talairach J. Co-planar stereotaxic atlas of the human brain-3-dimensional proportional system. An approach to cerebral imaging 1988.
31. Evans AC, Collins DL, Mills S, Brown ED, Kelly RL, Peters TM, editors. 3D statistical neuroanatomical models from 305 MRI volumes. 1993 IEEE conference record nuclear science symposium and medical imaging conference; 1993: IEEE.
32. Rex DE, Ma JQ, Toga AW. The LONI pipeline processing environment. Neuroimage 2003;19:1033-48.
33. Thompson PM, Mega MS, Woods RP, Zoumalan CI, Lindshield CJ, Blanton RE, Moussai J, Holmes CJ,

Cummings JL, Toga AW. Cortical change in Alzheimer's disease detected with a disease-specific population-based brain atlas. Cereb Cortex 2001;11:1-16.
34. Whitwell JL. Progression of atrophy in Alzheimer's disease and related disorders. Neurotox Res 2010;18:339-46.
35. Small BJ, Mobly JL, Laukka EJ, Jones S, Backman L. Cognitive deficits in preclinical Alzheimer's disease. Acta Neurol Scand Suppl 2003;179:29-33.
36. Zhao Y, Bhattacharjee S, Jones BM, Hill JM, Clement C, Sambamurti K, Dua P, Lukiw WJ. Beta-Amyloid Precursor Protein (betaAPP) Processing in Alzheimer's Disease (AD) and Age-Related Macular Degeneration (AMD). Mol Neurobiol 2015;52:533-44.
37. Okamura N, Harada R, Furumoto S, Arai H, Yanai K, Kudo Y. Tau PET imaging in Alzheimer's disease. Curr Neurol Neurosci Rep 2014;14:500.
38. Roh JH, Qiu A, Seo SW, Soon HW, Kim JH, Kim GH, Kim MJ, Lee JM, Na DL. Volume reduction in subcortical regions according to severity of Alzheimer's disease. J Neurol 2011;258:1013-20.
39. Kim J, Na HK, Byun J, Shin J, Kim S, Lee BH, Na DL. Tracking Cognitive Decline in Amnestic Mild Cognitive Impairment and Early-Stage Alzheimer Dementia: Mini-Mental State Examination versus Neuropsychological Battery. Dement Geriatr Cogn Disord 2017;44:105-17.
40. Peng GP, Feng Z, He FP, Chen ZQ, Liu XY, Liu P, Luo BY. Correlation of hippocampal volume and cognitive performances in patients with either mild cognitive impairment or Alzheimer's disease. CNS Neurosci Ther 2015;21:15-22.
41. Fox NC, Scahill RI, Crum WR, Rossor MN. Correlation between rates of brain atrophy and cognitive decline in AD. Neurology 1999;52:1687-9.

Cite this article as: Guo XY, Chang Y, Kim Y, Rhee HY, Cho AR, Park S, Ryu CW, Lee JS, Lee KM, Shin W, Park KC, Kim EJ, Jahng GH. Development and evaluation of a T1 standard brain template for Alzheimer' disease. Quant Imaging Med Surg 2021;11(6):2224-2244. doi: 10.21037/qims-20-710

Supplementary Tables

Table S1 Demographic Data and Neuropsychological Tests 2
Table S2 Brain Tissue Volumes Between the Left and Right Areas in Each ROI 3
Table S3 Voxel-Based Comparisons of GMV 4
A) Without separating gender 4
B) Only the Female 4
C) Only the Male 5
D) Comparison between female and male 6
Table S4 Voxel-Based Comparisons of WMV 7
A) Without separating gender 7
B) Only the Female 7
C) Only the Male 8
D) Comparison between female and male 8
Table S5 Voxel-Based Multiple Regression Analyses Between GMV and Age 9
A) Without separating gender 9
B) Only the Female 11
Table S6 Voxel-Based Multiple Regression Analyses Between WMV and Age 12
A) Without separating gender 12
B) Only the Female 13

http://dx.doi.org/10.21037/qims-20-710

Table S1 Information of four-cohort studies

Group		Cohort1 (Y2006)	Cohort2 (Y2009)	Cohort3 (Y2011)	Cohort4 (Y2014)	Total, mean or median
CN	N	43	36	16	16	111
	Age (year)	64.95±7.55	64.17±9.63	65.56±8.93	66.38±7.08	64.99±8.34
	Gender (M/F)	15/28	10/26	3/13	3/13	31/80
	K-MMSE	27.98±2.40	27.50±2.52	28.00±1.86	28.06±1.65	27.84±2.26
	CDR(range)	0(0-0.5)	0(0-0.5)	0(0-0.5)	0(0-0.5)	0(0-0.5)
MCI	N	43	24	18	16	101
	Age (year)	67.72±7.78	68.88±6.75	74.22±5.56	71.31±7.10	69.73±7.39
	Gender (M/F)	19/24	7/17	3/15	4/12	33/68
	K-MMSE	26.65±3.77	24.29±4.69	24.39±3.38	26.50±2.42	25.66±3.89
	CDR(range)	0.5(0-0.5)	0.5(0.5-1)	0.5(0.5-0.5)	0.5(0-0.5)	0.5(0-1)
AD	N	34	29	28	23	114
	Age(year)	72.47±9.30	75.83±7.51	74±8.10	77.35±7.53	74.68±8.33
	Gender(M/F)	7/27	7/22	4/24	4/19	22/92
	K-MMSE	17.44±4.84	18.38±4.87	16.89±5.20	18.09±5.96	17.68±5.14
	CDR(range)	1(0.5-2)	1(0.5-2)	1(0-2)	1(0.5-2)	1(0-2)

This table summarizes the demographic data and the result of the neuropsychological tests in participants with cognitively normal (CN) elderly, amnestic mild cognitive impairment (MCI), and Alzheimer's disease (AD) obtained from four different cohort studies.

The data of age and K-MMSE scores are presented as the mean ± standard deviation, but those of CDR scores are presented as the median (range) value.
K-MMSE, Korean version of the Mini-Mental State Examination; CDR, Clinical Dementi a Rating

 http://dx.doi.org/10.21037/qims-20-710

Table S2 Results of the comparisons of brain tissue volumes between the left and right areas

ROI		Left (mm^3)	Right (mm^3)	*P-value
Amygdala	CN	598.51±60.77	603.87±61.63	P = 0.1325
	MCI	545.77±90.24	550.08±88.45	P = 0.4553
	AD	420.42±79.55	427.42±83.42	P = 0.2848
	All	520.11±108.10	525.69±108.18	P = 0.0750
Parahippocampal Gyrus	CN	433.42±40.49	433.67±39.56	P = 0.8774
	MCI	402.45±49.40	402.44±51.22	P = 0.9976
	AD	327.77±41.22	328.77±42.05	P = 0.7238
	All	387.01±62.52	387.43±62.73	P = 0.7511
Posterior Cingulate	CN	325.25±41.04	325.64±38.00	P = 0.8487
	MCI	313.60±45.29	316.39±45.48	P = 0.2441
	AD	273.46±38.02	273.17±34.80	P = 0.8817
	All	303.66±47.03	304.60±45.72	P = 0.4423
Corpus callosum	CN	98.13±10.57	109.20±12.93	P < 0.0001
	MCI	96.20±11.61	109.13±12.81	P < 0.0001
	AD	94.92±16.45	107.18±17.04	P < 0.0001
	All	96.40±13.21	108.48±14.42	P < 0.0001
Anterior Cingulate	CN	308.44±37.15	298.12±33.92	P < 0.0001
	MCI	295.53±38.67	283.80±37.80	P < 0.0001
	AD	257.89±34.65	251.66±29.36	P = 0.0013
	All	286.86±42.60	277.48±38.97	P < 0.0001
Hippocampus	CN	501.89±51.49	515.94±51.58	P < 0.0001
	MCI	458.09±68.60	470.03±70.77	P = 0.0048
	AD	355.09±56.71	363.22±64.77	P = 0.0551
	All	437.14±85.17	448.49±89.95	P < 0.0001
Insula	CN	361.92±35.71	358.70±38.00	P = 0.0719
	MCI	350.47±41.96	343.49±40.86	P < 0.0001
	AD	307.82±34.58	302.97±32.06	P = 0.0062
	All	339.60±44.14	334.59±43.91	P < 0.0001
Precuneus	CN	313.64±31.62	304.93±30.06	P < 0.0001
	MCI	301.04±35.19	294.94±33.48	P = 0.0001
	AD	266.91±33.81	260.72±34.52	P = 0.0001
	All	293.47±38.93	286.48±37.83	P < 0.0001
Putamen	CN	370.57±42.81	380.16±41.75	P < 0.0001
	MCI	356.35±39.73	365.15±43.00	P = 0.0003
	AD	333.24±42.36	344.15±46.09	P < 0.0001
	All	353.10±44.33	362.89±46.01	P < 0.0001
Thalamus	CN	416.45±37.29	421.80±45.11	P = 0.0211
	MCI	393.54±51.39	396.33±58.76	P = 0.3656
	AD	355.22±46.25	351.72±51.78	P = 0.2095
	All	387.93±51.87	389.41±59.62	P = 0.3428

*P-value by paired samples t-test.

Data show mean ± standard deviation values. The entire corpus callosum was defined as a representative ROI for white matter.

ROI, region-of-interest; CN, cognitively normal; MCI, mild cognitive impairment; AD, Alzheimer's disease; All, the three groups together.

 http://dx.doi.org/10.21037/qims-20-710

Table S3 Results of the voxel-based comparisons of gray matter volume (GMV) among the three participant groups without separating the gender (3A), with only the female group (3B), with only the male group (3C), and comparison between the male and female groups (3D).

A) Without separating gender

Group analysis	Cluster size	Cluster location	BA	Talairach coordinates	Z score
CN>MCI					
	641	Rt middle temporal gyrus	21	53.22, -20.44, -8.92	6.386
		Rt insula	13	40.64, -21.02, -2.43	5.337
	1037	Lt medial globus pallidus		-16.14, -6.1, -8.74	6.335
		Lt parahippocampal gyrus	34	-24.32, 6.04, -17.18	5.556
	456	Lt parahippocampal gyrus	27, 35, 36	-10.86, -36.91, 3.3	5.863
	1624	Rt parahippocampal gyrus	30, 35	17.03, -31.95, -5.22	5.811
		Rt amygdala		26.9, -7.59, -9.5	5.745
CN>AD					
	221705	Lt amygdala		-17.52, -8.76, -10.36	65535
		Lt parahippocampal gyrus	34	-18.87, -0.24, -10.93	65535
		Rt amygdala		26.88, -9.12, -8.29	65535
	261	Lt cerebellar tonsil		-34.1, -64.27, -33.47	5.416
MCI>AD					
	180222	Rt anterior cingulate	32	3.39, 34.32, -4.58	65535
		Lt frontal subcallosal gyrus	34	-25.77, 4.25, -13.32	65535
		Lt amygdala		-18.89, -8.62, -11.72	65535

Rt, right; Lt, left; BA, Brodmann area

B) Only the Female

Group analysis	Cluster size	Cluster location	BA	Talairach coordinates	Z score
CN>AD					
	172463	Lt amygdala		-17.52, -8.76, -10.36	65535
		Lt frontal subcallosal gyrus	34	-25.74, 5.78, -14.53	65535
		Lt parahippocampal gyrus	34	-20.24, 1.3, -12.16	65535
MCI>AD					
	122110	Lt cingulate gyrus	31	-0.17, -27.66, 38.14	65535
		Rt occipital precuneus	31	1.31, -66.75, 19.6	65535
		Lt anterior cingulate	32	-4.93, 35.76, -4.58	65535
	677	Rt precentral gyrus	6	37.44, 1.88, 37.52	6.666
	213	Rt middle frontal gyrus	6	24.74, -5.08, 51.51	6.279
	178	Lt occipital cuneus	18	-4.23, -87.16, 12.16	5.839
	346	Lt precentral gyrus	6	-45.87, -6.07, 35.36	5.625

Rt, right; Lt, left; BA, Brodmann area

 http://dx.doi.org/10.21037/qims-20-710

C) Only the Male

Group analysis	Cluster size	Cluster location	BA	Talairach coordinates	Z score
CN>MCI					
	160	Lt anterior cingulate	32	-4.94, 34.37, -4.71	5.619
CN>AD					
	35526	Rt putamen		26.86, -9.25, -6.95	65535
		Lt anterior cingulate	32	-0.77, 34.34, -4.64	65535
		Rt medial globus pallidus		17.17, -6.27, -8.19	65535
	446	Lt thalamus, medial dorsal nucleus		-2.5, -12.06, 8.5	6.6857
		Rt thalamus	*	1.75, -16.89, 0	5.532
		Lt thalamus	*	0.37, -5.84, 2.38	5.081
	229	Rt fusiform gyrus	37	42.05, -59.24, -15.49	6.605
	312	Rt middle frontal gyrus	6	26.08, -9.54, 53.81	6.387
	451	Lt inferior temporal gyrus	20	-51.02, -57.89, -11.53	6.317
		Lt fusiform gyrus	37	-50.89, -43.26, -16.9	5.517
		Lt cerebellum culmen	*	-42.46, -38.46, -23.06	5.431
	454	Rt middle frontal gyrus	10	35.04, 47.18, 21.5	6.228
		Rt superior frontal gyrus	10	23.92, 49.9, 22.92	5.991
	458	Lt cingulate gyrus	31	-5.74, -27.76, 39.39	6.116
	157	Rt middle frontal gyrus	11	25.6, 39.67, -2.34	6.056
	331	Lt cingulate gyrus	31	-1.55, -57.74, 28.51	6.016
		Lt posterior cingulate	23	-5.59, -58.2, 18.94	5.273
	277	Rt middle temporal gyrus	39	47.15, -62.67, 19.41	6.005
		Rt superior temporal gyrus	39	52.62, -60.56, 26.46	5.509
	109	Lt superior temporal gyrus	39	-55.57, -60.74, 17.85	5.774
	140	Rt superior frontal gyrus	10	20.04, 57.47, 3.3	5.586
MCI>AD					
	3071	Rt amygdala		26.88, -7.72, -8.16	7.119
		Rt parahippocampal gyrus	28	15.8, -7.53, -9.68	7.041
	3356	Lt amygdala		-17.5, -8.63, -11.7	7.061
	1146	Rt anterior cingulate	24	2, 32.93, -4.73	6.935
		Rt caudate, caudate head		7.49, 13.21, -5.15	5.099
	286	Rt inferior parietal lobule	40	37.14, -38.68, 48.54	6.369
	186	Rt inferior temporal gyrus	37	54.42, -54.76, -4.04	6.150
	147	Lt caudate, caudate head		-2.34, 4.22, 0.58	5.906
	104	Lt inferior temporal gyrus	20	-51.02, -57.89, -11.53	5.905
	238	Lt insula	13	-42.63, -13.6, -3.14	5.882
		Lt superior temporal gyrus	22	-45.29, -3.16, -8.95	5.621
	124	Lt middle temporal gyrus	21	-49.12, -0.65, -34.45	5.722
		Lt inferior temporal gyrus	20	-43.65, -6.79, -29.54	5.125

Rt, right; Lt, left; BA, Brodmann area

 http://dx.doi.org/10.21037/qims-20-710

D) Comparison between female and male

Group analysis	Cluster size	Cluster location	BA	Talairach coordinates	Z score
CN: Female<Male					
	304	Lt middle temporal gyrus	38	-33.73, 2.85, -41.97	6.025
	225	Lt frontal precentral gyrus	6	-32.3, -11.16, 58.08	5.801
		Lt middle frontal gyrus	6	-26.76, -3.06, 61.64	5.504
	331	Rt middle temporal gyrus	38	45.35, 6.24, -36.25	5.762
		Rt superior temporal gyrus	38	32.9, 16.22, -36.87	5.302
	240	Lt limbic lobe, uncus	28	-17.34, -6.05, -23.62	5.635

CN, cognitively normal; MCI, mild cognitive impairment; AD, Alzheimer's disease; Rt, right; Lt, left; BA , Brodmann area

Subject's total intracranial volume (TIV), age, gender, and education-year were used as covariates. A significance level of $p = 0.01$ was applied with correction for multiple comparisons using the family-wise error (FWE) method and clusters with at least 50 contiguous voxels. In this list, we list the cluster areas, which have the cluster size of greater than 100.

 http://dx.doi.org/10.21037/qims-20-710

Table S4 Results of the voxel-based comparison of white matter volume (WMV) among the three participant groups without separating the gender (4A), with only the female group (4B), with only the male group (4C), and comparison between the male and female groups (4D).

A) Without separating gender

Group analysis	Cluster size	Cluster location	BA	Talairach coordinates	Z score
CN>MCI					
	1236	Rt frontal lobe, sub-gyral		21.45, 43.88, -2.01	7.106
	1214	Lt frontal lobe, sub-gyral		-23.16, 31.76, 8.25	6.656
	206	Rt middle temporal gyrus		49.17, -11.38, -14.89	5.772
		Rt temporal lobe, sub-gyral		38, -21.36, -13.32	5.441
	316	Lt frontal lobe, sub-gyral		-26.23, 20.03, 27.35	5.561
		Lt cingulate gyrus		-17.93, 21.12, 30.3	5.139
CN>AD					
	142102	Lt frontal lobe, sub-gyral		-20.4, 33.01, 9.76	65535
	286	Rt cerebellar tonsil		11.78, -51.67, -34.2	5.361
MCI>AD					
	116760	Lt frontal lobe, sub-gyral		-20.41, 34.27, 11.23	65535
		Rt frontal lobe, corpus callosum		13.07, 31.22, -2	65535

Rt, right; Lt, left; BA , Brodmann area

B) Only the Female

Group analysis	Cluster size	Cluster location	BA	Talairach coordinates	Z score
CN>AD					
	105204	Lt frontal lobe, sub-gyral		-21.81, 32.88, 11.08	65535
		Lt parietal lobe, sub-gyral		-29.28, -47.82, 28.98	65535
	117	Rt extra-nuclear		14.21, 4.75, 9.02	5.523
MCI>AD					
	73532	Lt frontal lobe, sub-gyral		-20.39, 35.8, 10.03	65535
		Rt limbic anterior cingulate		14.47, 31.34, -3.32	65535
		Lt frontal lobe, corpus callosum		-14.7, 29.96, -2.59	65535

Rt, right; Lt, left; BA, Brodmann area

 http://dx.doi.org/10.21037/qims-20-710

C) Only the Male

Group analysis	Cluster size	Cluster location	BA	Talairach coordinates	Z score
CN>MCI					
	130	Lt caudate head		-11.95, 18.77, -3.61	5.868
	180	Rt frontal lobe, sub-gyral		18.67, 42.5, -2.19	5.632
CN>AD					
	3777	Rt parahippocampal gyrus		25.56, -22.3, -17.67	6.580
		Rt temporal lobe, sub-gyral		39.45, -14.12, -15.31	6.251
	12074	Lt frontal lobe, sub-gyral		-20.38, 33.14, 8.42	65535
	14647	Rt frontal lobe, sub-gyral		21.24, 31.39, 10.31	7.795
		Rt caudate head		10.26, 18.65, -3.24	7.095
	3880	Lt temporal lobe, sub-gyral		-31.2, -3.06, -24.92	6.764
MCI>AD					
	495	Lt temporal lobe, sub-gyral		-42.69, -33.3, -3.65	5.806
	1093	Rt frontal lobe, sub-gyral		23.49, -17.74, 36.78	5.757
		Rt limbic cingulate gyrus		20.86, -2.97, 30.02	5.070
	579	Lt frontal lobe, sub-gyral		-26.45, -26.87, 31.01	5.707
	648	Rt frontal lobe, sub-gyral		19.85, 31.4, 10.29	5.548
		Rt limbic anterior cingulate gyrus		17.16, 37.53, 5.42	5.431
		Rt extra-nuclear		21.15, 23.88, 15.01	5.380
	161	Lt temporal lobe, sub-gyral		-32.59, -3.05, -24.94	5.531
		Lt limbic lobe, uncus		-32.62, 4.94, -20.13	5.010
	141	Rt limbic parahippocampal gyrus		25.52, -23.96, -15.13	5.275
	185	Rt extra-nuclear		19.93, -47.42, 23.08	5.346
		Rt parietal lobe, sub-gyral		27.72, -46.06, 23.35	5.166
	171	Lt frontal lobe, sub-gyral		-18.88, 42.17, 2.55	5.303

Rt, right; Lt, left; BA, Brodmann area

D)Comparison between female and male

Group analysis	Cluster size	Cluster location	BA	Talairach coordinates	Z score
CN: Female<Male					
	144	Rt middle frontal gyrus		24.81, -4.56, 46.15	5.223
		Rt frontal lobe, sub-gyral		27.51, 0.37, 53.42	5.186
MCI: Female<Male					
	9316	Lt brainstem, midbrain		-0.88, -33.61, -16.49	5.196

CN, cognitively normal; MCI, mild cognitive impairment; AD, Alzheimer's disease; Rt, right; Lt, left; BA , Brodmann area

Subject's total intracranial volume (TIV), age, gender, and education-year were used as covariates. A significance level of $p = 0.01$ was applied with correction for multiple comparisons using the family-wise error (FWE) method and clusters with at least 50 contiguous voxels. In this list, we list the cluster areas, which have the cluster size of greater than 100.

 http://dx.doi.org/10.21037/qims-20-710

Table S5 Results of the voxel-based multiple regression analyses between gray matter volume (GMV) and age in each participant group without separating the gender (5A) and with only the female group (5B).

A) Without separating gender

Group analysis	Cluster size	Cluster location	BA	Talairach coordinates	Z score
CN: (-) Age					
	1761	Rt insula	13	37.69, -20.92, 11.04	7.031
		Rt superior temporal gyrus	41	50.08, -27.23, 17.41	6.728
		Rt inferior parietal lobule	40	51.29, -28.54, 30.82	5.260
	1020	Rt cerebellum, culmen		22.77, -29.27, -18.38	6.603
	577	Rt thalamus, pulvinar		11.3, -33.23, 8.08	6.603
		Rt parahippocampal gyrus	27	12.82, -32.32, -1.27	6.008
		Rt thalamus		7.07, -21.41, 17.23	5.007
	2534	Rt limbic anterior cingulate	25	1.85, 0.27, -2.42	6.518
		Lt parahippocampal gyrus	36	-23.12, -32.35, -14.04	6.451
		Lt cerebellum, culmen		-19.05, -42.68, -9.55	6.390
	523	Rt cerebellum, culmen		38.01, -45.99, -21.06	6.401
	1445	Rt limbic posterior cingulate	30	4.24, -60.13, 9.46	6.376
		Lt occipital cuneus	30	-6.86, -65.54, 7.41	6.211
	368	Lt cerebellum, declive		-46.71, -55.47, -22.04	6.171
		Lt cerebellum, culmen		-41.1, -46.85, -23.83	5.263
	284	Lt limbic cingulate gyrus	31	-5.76, -27.89, 40.72	5.987
	228	Lt thalamus		-1.16, -15.13, 10.93	5.766
	388	Rt inferior frontal gyrus	47	36.76, 34.54, -8.04	5.705
		Rt insula	13	39.39, 19.77, -1.29	5.358
	144	Lt limbic, anterior cingulate	32	-0.77, 35.74, -4.51	5.616
	447	Rt inferior temporal gyrus	20	58.77, -43.83, -15.1	5.612
		Rt middle temporal gyrus	37	54.47, -54.37, -8.06	5.535
	162	Lt inferior frontal gyrus	47	-25.74, 7.18, -14.4	5.508
MCI: (-) Age					
	49437	Lt parahippocampal gyrus	34	-20.22, 2.83, -13.36	65535
		Lt amygdala		-18.93, -10.28, -9.18	65535
		Lt putamen		-27.28, -11.76, -8.11	65535
	847	Rt middle frontal gyrus	46	41.98, 34.83, 17.75	7.424
		Rt inferior frontal gyrus	46	44.9, 35.86, 7.08	5.821
	425	Rt occipital	19	41.96, -68.15, -10.93	6.656
	1788	Rt middle occipital gyrus		26.47, -88.94, 0.35	6.497
		Rt middle temporal gyrus	39	48.62, -64.82, 12.47	6.043
	2269	Lt occipital lobe, precuneus	31	-29.3, -73.98, 22.45	6.345
		Lt middle occipital gyrus	19	-30.51, -80.92, 6.91	6.276
	378	Lt medial frontal gyrus	9	-10.85, 44.1, 25.84	6.112
		Lt medial frontal gyrus	10	-10.71, 49.2, 16.87	5.639
	140	Lt parietal postcentral gyrus	2	-36.32, -25.2, 43.16	6.104
	302	Lt middle frontal gyrus	46	-41.42, 28.88, 23.88	6.059
	347	Lt thalamus		-1.13, -9.41, 10.12	6.058
	958	Lt cerebellum, uvula		-21.74, -69.44, -24.29	6.027
		Lt cerebellum, declive		-24.63, -79.86, -18.57	5.930
	233	Rt superior temporal gyrus	22	49.01, 6.62, 3.03	6.021

 http://dx.doi.org/10.21037/qims-20-710

		Rt frontal precentral gyrus	6	48.91, -3.68, 7.46	5.076
	237	Rt middle frontal gyrus	10	31.17, 52.08, 0.28	5.663
		Rt superior frontal gyrus	10	26.88, 51.19, 9.58	5.429
	160	Lt superior temporal gyrus	41	-45.72, -36.51, 14.91	5.563
	202	Rt inferior frontal gyrus	47	25.57, 28.49, -3.4	5.443
		Rt middle frontal gyrus	47	32.56, 35.7, -5.3	5.247
AD: (-) Age					
	487	Lt cerebellum, uvula		-17.59, -73.65, -24.62	5.543
		Lt cerebellum, culmen		-31.4, -60.74, -26.33	5.320
All Group: (-) Age					
	190935	Rt limbic parahippocampal gyrus	27	11.35, -34.23, 3.93	65535
		Lt limbic anterior cingulate	25	-0.94, 1.55, -1	65535
		Lt limbic parahippocampal gyrus	27	-13.64, -35.5, 3.39	65535
	166	Lt inferior parietal lobule	40	-33.64, -53.29, 41.9	5.311

 http://dx.doi.org/10.21037/qims-20-710

B) Only the Female

Group analysis	Cluster size	Cluster location	BA	Talairach coordinates	Z score
CN: (-) Age					
	1089	Rt superior temporal gyrus	41	40.33, -34.29, 17.93	6.312
		Rt insula	13	36.3, -22.31, 10.89	5.745
	308	Rt thalamus	*	9.93, -34.49, 6.58	6.150
	251	Lt occipital lingual gyrus	18	-9.59, -61.07, 5.09	5.740
	151	Rt cerebellum, culmen	*	25.56, -27.76, -19.54	5.648
	100	Rt insula	13	37.97, 20.91, 1.5	5.410
MCI: (-) Age					
	8290	Rt parahippocampal gyrus	34	20.04, -11.09, -16.7	7.299
		Rt temporal lobe, sub-gyral	21	39.42, -3.33, -10.24	6.806
		Rt parahippocampal gyrus	27	12.79, -35.25, -0.2	6.757
	3942	Rt occipital lingual gyrus	18	1.52, -78.9, -0.47	7.057
		Lt occipital cuneus	30	-6.85, -62.74, 7.68	6.214
		Rt cingulate gyrus	31	2.65, -38.33, 31.77	6.124
	4534	Lt putamen		-27.3, -11.89, -6.77	6.974
		Lt frontal subcallosal gyrus	34	-21.6, 4.23, -13.25	6.764
	1179	Rt limbic anterior cingulate	25	0.43, 1.41, 0.36	6.874
		Lt limbic anterior cingulate	32	-0.77, 35.74, -4.51	6.365
		Lt medial frontal gyrus	10	-6.22, 42.01, -10.77	5.098
	1086	Lt insula	13	-34.34, 14.78, 9.15	6.534
	346	Rt middle frontal gyrus	46	40.62, 32.3, 14.78	6.251
	286	Rt cerebellum, declive	*	12.86, -75.86, -17.56	6.071
	319	Lt cerebellum, declive	*	-41.15, -54.1, -21.81	6.061
	181	Rt medial frontal gyrus	9	9.87, 29.49, 30.21	5.975
	465	Rt transverse temporal gyrus	41	43.18, -30.99, 12.88	5.725
		Rt insula	13	44.42, -34.84, 23.35	5.445
		Rt inferior parietal lobe	40	55.49, -31.09, 27.94	5.345
	150	Rt occipital fusiform gyrus	19	41.94, -68.28, -9.59	5.644
	160	Lt middle occipital gyrus	19	-30.67, -73.84, 21.09	5.568
	114	Rt insula	13	32.29, 18.63, 10.64	5.351

CN, cognitively normal; MCI, mild cognitive impairment; AD, Alzheimer's disease; Rt, right; Lt, left; BA , Brodmann area

Subject's total intracranial volume (TIV), gender, and education-year were used as covariates. (-) indicates the negative correlation. A significance level of $p = 0.01$ was applied with correction for multiple comparisons using the family-wise error (FWE) method and clusters with at least 50 contiguous voxels. In this list, we list the cluster areas, which have the cluster size of greater than 100. For only the male, there are no correlations between GMV and age for all three participant groups.

 http://dx.doi.org/10.21037/qims-20-710

Table S6 Results of the voxel-based multiple regression analyses between white matter volume (WMV) and age in each participant group without separating the gender (6A) and with only the female group (6B).

A) Without separating gender

Group analysis	Cluster size	Cluster location	BA	Talairach coordinates	Z score
CN: (-) Age					
	148	Lt limbic cingulate gyrus		-9.83, -25.82, 34.1	5.521
	146	Rt inferior parietal lobule		37.41, -36.72, 28.46	4.968
MCI: (-) Age					
	64925	Lt temporal lobe, sub-gyral		-28.79, -30.45, -4.5	65535
		Rt frontal lobe, sub-gyral		26.68, 33.25, 20.04	65535
		Lt frontal lobe, sub-gyral		-16.07, 24.64, -5.82	7.774
	466	Lt parahippocampal gyrus		-27.18, -19.23, -18.27	6.277
AD: (-) Age					
	328	Rt extra-nuclear		25.33, -30.86, -2.27	6.225
	149	Lt medial frontal gyrus		-11.21, 18.12, 46.34	5.894
	3130	Rt limbic anterior cingulate		12.97, 41.48, 8.43	5.812
		Rt frontal lobe, sub-gyral		23.84, 31.47, 23.88	5.533
	2219	Lt frontal lobe, sub-gyral		-26.13, 30.33, 22.92	5.772
		Lt limbic anterior cingulate		-9.23, 36.14, 6.19	5.480
		Lt sub-lobar, extra-nuclear		-21.65, 27.2, -2.97	5.314
	342	Lt frontal lobe, sub-gyal		-27.8. -10.09. 32.58	5.339
	221	Rt brainstem, midbrain		12.98, -7.78, -7.05	5.322
	149	Rt frontal lobe, sub-gyral		24.84, -19.41, 39.34	5.105
All Group: (-) Age					
	146355	Rt limbic lobe, sub-gyral		23.96, -29.32, -3.5	65535
		Lt limbic parahippocampal gyrus		-27.4, -30.45, -4.48	65535
		Lt frontal lobe, sub-gyral		-24.66, 30.98, 16.25	65535

 http://dx.doi.org/10.21037/qims-20-710

B) Only the Female

Group analysis	Cluster size	Cluster location	BA	Talairach coordinates	Z score
CN: (-) Age					
	127	Rt temporal lobe, sub-gyral		39.25, -34.73, -6.46	5.170
MCI: (-) Age					
	9559	Lt frontal lobe, sub-gyral		-16.07, 24.64, -5.82	7.396
		Lt limbic anterior cingulate		-17.63, 35.66, 11.41	6.221
		Lt limbic cingulate gyrus		-15.18, 19.58, 31.55	6.138
	11065	Rt frontal lobe, sub-gyral		24.16, 39.28, 1.65	7.384
		Rt limbic lobe, anterior cingulate		7.51, 31.24, -2.09	7.159
	496	Lt temporal lobe, sub-gyral		-28.79, -30.45, -4.5	6.849
	180	Rt limbic lobe, sub-gyral		23.96, -29.32, -3.5	6.629
	2564	Rt temporal lobe, sub-gyral		34.62, -61.47, 22.01	6.359
		Rt parietal lobe, sub-gyral		23.52, -54.55, 23.83	5.703
	263	Rt occipital fusiform gyrus		32.31, -51.2, -10.84	6.013
	1026	Lt limbic, cingulate gyrus		-13.99, -31.26, 32.16	5.988
		Lt parietal lobe, precuneus		-16.85, -51.07, 32.94	5.897
	279	Rt limbic parahippocampal gyrus		25.57, -19.51, -17.41	5.659
	184	Rt temporal lobe, sub-gyral		40.75, -21.64, -10.6	5.501
	355	Lt temporal lobe, sub-gyral		-26.43, -58.23, 19.93	5.427

CN, cognitively normal; MCI, mild cognitive impairment; AD, Alzheimer's disease; Rt, right; Lt, left; BA , Brodmann area

Subject's total intracranial volume (TIV), gender, and education-year were used as covariates. A significance level of $p = 0.01$ was applied with correction for multiple comparisons using the family-wise error (FWE) method and clusters with at least 50 contiguous voxels. In this list, we list the cluster areas, which have the cluster size of greater than 100. For only the male, there are no correlations between WMV and age for all three participant groups.

 http://dx.doi.org/10.21037/qims-20-710